



This is a repository copy of *Cellular rearrangement of the prechordal plate contributes to eye degeneration in the cavefish*.

White Rose Research Online URL for this paper:
<http://eprints.whiterose.ac.uk/136995/>

Version: Accepted Version

Article:

Ren, X., Hamilton, N. orcid.org/0000-0002-3299-9133, Müller, F. et al. (1 more author) (2018) Cellular rearrangement of the prechordal plate contributes to eye degeneration in the cavefish. *Developmental Biology*, 441 (2). pp. 221-234. ISSN 0012-1606

<https://doi.org/10.1016/j.ydbio.2018.07.017>

Article available under the terms of the CC-BY-NC-ND licence
(<https://creativecommons.org/licenses/by-nc-nd/4.0/>).

Reuse

This article is distributed under the terms of the Creative Commons Attribution-NonCommercial-NoDerivs (CC BY-NC-ND) licence. This licence only allows you to download this work and share it with others as long as you credit the authors, but you can't change the article in any way or use it commercially. More information and the full terms of the licence here: <https://creativecommons.org/licenses/>

Takedown

If you consider content in White Rose Research Online to be in breach of UK law, please notify us by emailing eprints@whiterose.ac.uk including the URL of the record and the reason for the withdrawal request.



eprints@whiterose.ac.uk
<https://eprints.whiterose.ac.uk/>

Cellular rearrangement of the prechordal plate contributes to eye degeneration in the cavefish

Xiaoyun Ren^{1,3,*}, Noémie Hamilton^{1,4,*}, Ferenc Müller²
and Yoshiyuki Yamamoto¹

¹ Department of Cell and Developmental Biology, University College London, London, United Kingdom

² Institute of Cancer and Genomics Sciences, College of Medical and Dental Sciences, University of Birmingham, Birmingham, United Kingdom

³ Current address: Institute of Environmental Science and Research, Porirua 5022, New Zealand

⁴ Current address: The Bateson Centre, University of Sheffield, S10 2TN, United Kingdom

* These authors contributed equally to this work.

Corresponding author.: yoshiyuki.yamamoto@ucl.ac.uk

Abstract

Astyanax mexicanus consists of two different populations: a sighted surface-dwelling form (surface fish) and a blind cave-dwelling form (cavefish). In the cavefish, embryonic expression of *sonic hedgehog a (shha)* in the prechordal plate is expanded towards the anterior midline, which has been shown to contribute to cavefish specific traits such as eye degeneration, enhanced feeding apparatus, and specialized brain anatomy. However, it is not clear how this expanded expression is achieved and which signaling pathways are involved.

Nodal signaling has a crucial role for expression of *shh* and formation of the prechordal plate. In this study, we report increased expression of prechordal plate marker genes, *nodal-related 2 (ndr2)* and *goosecoid (gsc)* in cavefish embryos at the tailbud stage. To investigate whether Nodal signaling is responsible for the anterior expansion of the prechordal plate, we used an inhibitor of Nodal signaling and showed a decreased anterior expansion of the prechordal plate and increased *pax6* expression in the anterior midline in treated cavefish embryos. Later in development, the lens and optic cup of treated embryos were significantly larger than untreated embryos. Conversely, increasing Nodal signaling in the surface fish embryo resulted in the expansion of anterior prechordal plate and reduction of *pax6* expression in the anterior neural plate together with the formation of small lenses and optic cups later in development. These results confirmed that Nodal signaling has a crucial role for the anterior expansion of the prechordal plate and plays a significant role in cavefish eye development. We showed that the anterior expansion of the prechordal plate was not due to increased total cell number, suggesting the expansion is achieved by changes in cellular distribution in the prechordal plate. In addition, the distribution of presumptive prechordal plate cells in Spemann's organiser was also altered in the cavefish. These results suggested that changes in the cellular arrangement of Spemann's organiser in early gastrulae could have an essential role in the anterior expansion of the prechordal plate contributing to eye degeneration in the cavefish.

Introduction:

Being able to adapt to specific environments is important to the survival of any species. In closely related organisms, this adaptability is evident in the diversification of morphology as well as behaviour. This is especially evident when species evolve by adaptation to conditions found in isolated extreme environments. Cave animals—trogllobites evolved in constant darkness—often show convergent physiological and phenotypic modifications: most lack pigments and eyes; but other sensory systems are often expanded (Jeffery, 2008; Protas and Jeffery, 2012).

The troglobite fish: Mexican tetra *Astyanax mexicanus*, has conspecific surface and several cave-dwelling populations (Hecht et al., 1988). The cave population shows regressive features such as loss of eye and pigmentation, and also adaptive features such as wider jaw and increased taste bud density (Jeffery, 2008; Yamamoto et al., 2009). Though the adult cavefish lacks eyes, cavefish embryos form small optic cups, which undergo degeneration during later juvenile stages. The morphogen sonic hedgehog (Shh) is a major regulator of the eyeless phenotype (Pottin et al., 2011; Yamamoto et al., 2004). *shha* expression along the anterior midline is expanded in embryos of the cave population. Artificially increasing *shha* expression in surface fish embryos phenocopies the developmental progression of eye degeneration seen in cave populations, namely, smaller optic cups, followed by lens apoptosis and the eventual degeneration of the eye (Yamamoto et al., 2004). *shha* expansion during cavefish embryogenesis also controls other morphological features such as wider jaw, increased taste bud density, a larger olfactory placode, and also a larger hypothalamus in larvae (Hinaux et al., 2016; Menuet et al., 2007; Yamamoto et al., 2009). Thus, the expanded expression of *shha* may be an important adaptive change gained during cavefish evolution. However, it is still unclear precisely how altered *shha* expansion is achieved and how its expansion controls eye degeneration in the cavefish.

There are at least three mechanisms that may explain the expanded expression of *shha* seen in cavefish.: 1) changes in cis-regulatory elements regulating *shha* expression along the anterior midline of cavefish embryos. A published quantitative trait loci (QTL) analysis suggested 12 loci in the cavefish genome are involved in eye degeneration. However, none of them is found near the *shha* gene on the linkage map (Gross et al., 2008; Protas et al., 2008, 2007). This suggests altered cis-regulatory elements are unlikely to have any influence on the expanded expression of *shha* and

resultant eye degeneration in the cavefish. 2) An increase in expression of an upstream regulator gene could directly cause an expanded expression of *shha*. 3) The distribution of *shha*-expressing cells is altered in cavefish embryos. For instance, *shha*-expressing cells in the posterior midline might migrate anteriorly during gastrulation, thus increasing cell numbers at the anterior midline.

Signaling molecules from the prechordal plate, which resides at the midline, positioned underneath the neural plate, pattern the ventral midline of the neural plate (Placzek and Briscoe, 2005; Wilson and Houart, 2004). Failure to pattern the prechordal plate correctly often leads to holoprosencephaly—malformation of the forebrain—one of the most common birth defects found in humans (Geng et al., 2009). In zebrafish, a member of the transforming growth factor β (TGF- β) family: *ndr2* (nodal-related 2; previously named *cyclops*) is a crucial regulator of prechordal plate patterning and *shha* expression in the anterior midline (Chen and Schier, 2002; Dougan, 2003; Gritsman et al., 2000; Hagos and Dougan, 2007; Müller et al., 2000; Sampath et al., 1998). Nodal also acts upstream of *shha* to pattern the fate of the floor plate, hypothalamus, and ventral telencephalon (Rohr et al., 2001; Tian et al., 2003). Therefore, the patterning of the prechordal plate and *ndr2* expression could be critical regulators of the anterior expansion of *shha* expression found in cavefish.

In this study, we set out to examine whether the prechordal plate is a regulator of eye degeneration in cavefish. We used prechordal plate markers, *ndr2*, *gsc*, and *dickopf-1* (*dkk1*) to examine the distribution of the anterior midline in *Astyanax* and found that the prechordal plate is indeed expanded in the cave population. Interestingly, cell number is not significantly different between cave and surface populations. Instead, the anterior expansion is achieved by cellular redistribution: more cells in the anterior and fewer cells in the posterior prechordal plate. By inhibiting or enhancing Nodal signaling in *Astyanax* embryos, we were able to increase or decrease eye size in cave and surface fish, respectively. We also describe an antagonistic relationship between the anterior expansion of the prechordal plate and the expression of *pax6* in the anterior midline. Moreover, the antagonistic relationship controls the ratio between the retina and non-retinal tissues (optic stalk or forebrain) in the anterior neural plate (ANP). These results support the idea that the cellular distribution of the prechordal plate is modified in the cavefish embryo and that anterior expansion of the prechordal plate has a crucial role in the eye development. In addition, we describe how the cellular distribution of presumptive prechordal plate cells in Spemann's organiser is altered in cavefish. We

propose a hypothesis that, in cavefish, altered cellular distribution in Spemann's organiser changes prechordal plate morphogenetic cell movements during gastrulation, the resultant change in cellular distribution leads to the anterior expansion of *shha* expression and thus the eye degeneration found in cavefish.

Material and Methods:

***Astyanax* and Embryo Culture**

Astyanax mexicanus surface and cavefish embryos were obtained by natural spawning or *in vitro* fertilisation of laboratory colonies. *Astyanax* from two cave populations is used in this study, the Tinaja cave and the Pachón cave. Adult fish were reared under conditions described by Jeffery and Martasian (Jeffery and Martasian, 1998). Embryos were cultured at 25°C in zebrafish embryo medium 2 (E2, Westerfield, 2000).

***In situ* hybridization and cell counting**

In situ hybridization using antisense RNA probes was carried out as previously described (Strickler et al., 2001). Two-colour *in situ* was performed with the following modifications. Fluorescein (FITC) or digoxigenin (DIG) labelled RNA probes (Roche) were incubated together in the initial hybridization step at 65°C. In general, FITC labelled probes were developed first using NBT/BCIP (5-bromo-4-chloro-3-indolyl-phosphate/4-nitro blue tetrazolium chloride, Roche) as the substrate for the AP labelled antibody, either at room temperature (RT) or overnight at 4°C. To stop the first reaction, embryos were washed in PBS and fixed with 4% paraformaldehyde in PBS for 30 minutes at RT. To further reduce the likelihood of cross-reaction, the enzymatic activity of the first antibody was quenched by washing the embryos with 0.2M glycine (pH2.0) for 30mins at RT. To develop the second probe, embryos were blocked (5% normal sheep serum, 2mg/ml BSA, 0.1% Tween, 1xPBS) a second time and incubated with anti-DIG AP antibody and developed using BCIP as the substrate. BCIP alone produces a cyan colour, where NBC/BCIP combined produces a dark blue colour.

To count the number of cells expressing *shha* or *gsc*, embryos of similar size and stage were selected. Stage of development was judged by the pattern of *paired box gene 2* (*pax2*) expression; its probe is always included in the hybridization cocktail. After *in situ* hybridization, embryos were dehydrated into 100% ethanol and embedded in 100% polyester wax. 10µm sections were cut from the animal-dorsal direction. Sections were secured to glass slides using 0.3% gelatine solution, rehydrated and counterstained with nuclei stain Hoechst. Sections were photographed using a compound microscope. Images were converted to grey scale, and the area of interest was isolated using Photoshop (Adobe Inc, USA). To count the cells, grey scale images

were converted to binary by thresholding and counted using the particle counting tool in ImageJ (NIH, USA).

Drug treatment and mRNA injections

Between 15 to 20 embryos were treated with 5ml of 25 μ M SB-431542 (Sigma, SB stock made in DMSO) dissolved in E2 in 6 well plates. Control sibling embryos were treated with the same concentration of DMSO. To wash off the drug after treatment, control and experimental embryos were washed several times with fresh E2.

Constitutively active Mothers against decapentaplegic homolog 2 (*smad2CA*) mRNA for injection was generated using an Sp6 mMessage Machine kit (Ambion) and was pressure injected into one cell stage embryos as previously described (Müller et al., 2000; Yamamoto et al., 2004). Control embryos were injected with an equivalent amount of *nGFP* mRNA.

Eye and lens measurements

48hr larvae were anaesthetised in 0.16mg/ml of MS222 (Tricaine methanesulfonate, Sigma, A5040) in E2 and held in place with 0.2% agar E2 solution. Photographs were taken using a Nikon dissection microscope with 8x magnification. Eye and lens areas were measured using the area tool in ImageJ software (NIH, USA).

Acridine orange staining

Anaesthetised live embryos were stained with acridine orange solution (20 μ g/ml in E2) for 20 mins at 25°C, washed three times with fresh E2. Embryos were further anaesthetised, held in position with 0.2% agar in E2 and photographed under a fluorescent dissecting microscope.

Lineage Analysis

Embryos were dechorionated by incubating in 0.1mg/ml pronase (Sigma-Aldrich) in E2 solution for 1 min. To label the anterior neural plate with Dil, fine glass needles were coated with Dil solution (25mg/ml Ethanol) by putting a small drop of Dil on the glass needle while resting on a glass slide and allowed to dry. Tailbud to 3 somite stage embryos were held in place by placing the embryo in 0.2% Agar. The Dil coated needle was gently inserted into position using a micromanipulator and was held in place for 30 seconds to allow Dil to stain the surrounding tissue. Immediately after labelling, a photograph of the anterior neural plate was taken at 10x magnification to document the

position of the label. After labelling, embryos were incubated in E2 until 24hrs post fertilisation, at this time tissues that received the label were photographed.

The final tissues labelled were classified as either eye, optic stalk, forebrain, nose or skin epidermis. Most Dil labelled cells in the forebrain were located either in the telencephalon or hypothalamus with most of them located ventrally. However, in our system, it is difficult to distinguish specific areas of the brain. All labelled cells around the telencephalon and hypothalamus are scored as “forebrain”. Embryos containing only epidermal staining were discarded.

To practice the labelling technique, especially to ensure we were consistently labelling positions corresponding to the most anterior midline of paired box protein 6 (*pax6*) expression pattern, the Dil labelling was photo-converted to the dark non-diffusible product by incubating with DAB and illuminating with rhodamine filtered UV light through a 20X objective. After conversion, *in situ* hybridization was performed as described using the *pax6* probe.

Quantitative PCR (qPCR)

Total RNA was extracted from 20 embryos for each sample by using TRIzol reagent (Invitrogen), and cDNA was synthesised using Superscript II (Invitrogen) enzyme using a poly-dT primer following the manufacturer’s protocol. Each sample was analysed by qPCR in triplicate using SYBR Green JumpStart *Taq* ReadyMix (Sigma) and specific primers (listed below). Δ CT was calculated using Ribosomal protein L13a (*rpl13a*) as a reference gene. Relative expression levels were plotted after determining $\Delta\Delta$ Ct by normalizing to a single sample with a high Δ CT value.

Primers were designed using Primer Express (v 2.0, Applied Biosystems) and published *A. mexicanus* sequence (see below). The qPCR products and efficiency of qPCR primers were verified by melt curve analysis. Primers were 18–30 nucleotides in length with a melting temperature between 58–64 °C. The primer sequences were as follows: *ndr2* (XM_007242927.3) forward primer, 5'-CAACCAGATTGGATGGGGCT-3' and reverse primer, 5'-TCTGCATGTAGGCGTGGTTT-3'; *ndr1* (XM_007256760.2) forward primer, 5'-CTTGGAAAGGGCTGCCAATG-3' and reverse primer, 5'-TACCGCTTCACGCACTTTCT-3'; *dkk1* (XM_007233996.1) forward primer, 5'-CACTGCAACAACGGAGTGTG-3' and reverse primer, 5'-CAGTACCAGTGTGGCGTTCT-3'; *gsc* (XM_007232124.1) forward primer, 5'-

TACACGTACAGGGACCGAGT-3' and reverse primer, 5'-
TAGCCTGTGGGAATGCAAGG-3'; rpl13a (XM_007244599.3) forward primer, 5'-
TCTGGAGGACTGTAAGAGGTATGC-3' and reverse primer, 5'-
AGACGCACAATCTTGAGAGCAG-3'.

Results:

Expanded *shha* expression is correlated with a reduction of *pax6* expression in the anterior neural plate.

Pax6 is a paired-class homeodomain transcription factor expressed in the embryonic central nervous system with important roles in the eye, brain and spinal cord formation in vertebrates (Ashery-Padan and Gruss, 2001; Gehring, 2005). Pax6 is expressed in the ANP which represents the future fore- and midbrain field in teleost (Loosli et al., 1998; Macdonald and Wilson, 1997; Strickler et al., 2001). The anterior domain of *pax6* expression corresponds to the eye field, and the posterior domain marks the prospective diencephalon. A small expression gap can be seen along the midline at the early tailbud stage (Loosli et al., 1998; Nornes et al., 1998; Strickler et al., 2001). During early somitogenesis stages, *pax6* is also expressed in the presumptive lens epithelium in two arcs, one on each side of the *pax6* expression in the ANP. As reported before, we found that the *pax6* expression area in the ANP is smaller in the cavefish when compared to surface fish (Figs. 1A, B); the expression gap along the midline is also wider, especially at the most anterior domain, when compared to the eyed surface fish ((Strickler et al., 2001), arrows in Figs. 1A, B). The expression intensity in the presumptive lens epithelium is weaker in cavefish when compared with that of the surface fish, and the expression also has a gap at the anterior midline, with a wider gap also been reported in the cavefish (Hinaux et al., 2016), arrowheads in Figs. 1A, B, surface fish n=17, Pachón n=17).

How this wider gap observed in the *pax6* expression domain of the cavefish is related to *shha* expression expansion ((Figs. 1G-I) is not clear. To examine the possible link between the expanded expression of *shha* and the expression gap of *pax6*, we performed two-colour *in situ* hybridization for *shha* and *pax6*. In surface fish, the anterior edges of *pax6* and *shha* expression were almost at the same anterior-posterior level. However, the anterior edge of *pax6* in the Pachón cavefish was always more posterior than that of *shha* (arrowheads, Figs. 1C, D surface n=9, Pachón n=13). Lateral views of the embryos also showed that the most anterior part of the *pax6* expression in the cavefish was located more posteriorly than that of the surface fish, indicating that anterior expression of *pax6* is reduced in the cavefish (arrowheads, Figs. 1C', D'). We also observed that the wider gap between the anterior *pax6* expression matched the

expanded *shha* expression in the cavefish embryos (Figs. 1A-D'). This data suggests that the expanded midline signaling of *shha* in the Pachón cavefish could be associated with down-regulation of *pax6* along the anterior midline in the ANP.

Cavefish has an expanded prechordal plate compared to surface fish

One mechanism for achieving an expanded expression of *shha* in the midline is the expansion of the prechordal plate itself. To examine whether the prechordal plate was expanded in cavefish embryos, we compared the expression pattern of prechordal plate marker genes, *gsc* and *ndr2* (previous name *cyclops*) between surface fish and cavefish. *gsc* is a paired homeobox family transcription factor and a prechordal plate marker in vertebrates (Niehrs et al., 1993; Schulte-Merker et al., 1994). In zebrafish, *ndr2* encodes a Nodal-related signaling protein, a member of TGF- β family, which is a crucial regulator of *shh* midline expression and prechordal plate formation. It is expressed in the prechordal plate of zebrafish embryos, along with the anterior midline at tailbud stages (Rebagliati et al., 1998; Sampath et al., 1998)

In the cavefish embryos, *gsc* was expressed in a 'salt and pepper' manner along the anterior midline in a wedge shape with its widest point at the most anterior region. Compared to the surface fish, the cells were more dispersed, and the expression domain was shorter and wider in the cavefish embryo along the anterior-posterior axis (Figs. 1E, F). We compared *gsc* expression between surface fish and Pachón cavefish and found that the expression domain in cavefish embryos (Pachón cave) was 30% larger than that of surface fish. *gsc* expression domain area was divided by that of the *pax2* expression domain to normalize for embryonic size differences (*gsc/pax2*, surface 0.751 ± 0.123 n=10; Pachón 0.979 ± 0.182 n=15; t-test $p < 0.01$, Fig. 1M).

ndr2 expression in *Astyanax* was not uniform along the entire prechordal plate but can be divided into anterior and posterior domains. The anterior domain consisted of the anterior tip expression (polster), which was denser and wider than the posterior domain. *ndr2* expression was wider in the two cavefish populations (Tinaja and Pachón cave) examined, especially in the anterior domain (arrowheads, Figs. 1J-L). To quantify this difference between the surface fish and Pachón cavefish, we measured the *ndr2* expression areas. In Pachón cavefish, *ndr2* expressing area was 50% larger than in the surface fish (*ndr2/pax2*, surface fish 0.53 ± 0.01 , n=20; Pachón cavefish 0.82 ± 0.01 , n=20; t-test $p < 0.001$, Fig. 1M).

These results suggest that the prechordal plate is also expanded at the anterior midline of cavefish when compared to surface fish.

Cavefish prechordal plate expansion is not due to an increase in cell number but rather cellular redistribution.

The expanded prechordal plate could be a result of increased cell number or cellular rearrangement. To distinguish between these two possibilities, we compared the number of cells expressing *shha* and *gsc* between the surface fish and Pachón cavefish at tailbud stage. We found that cell numbers in the prechordal plate were not significantly different (*shha*; Surface 373 ± 63 $n=9$; Pachón 365 ± 73 $n=9$, t-test $p > 0.05$, *gsc*; Surface 401 ± 70 $n=11$; Pachón 413 ± 95 $n=9$, t-test $p > 0.05$, Fig. 1N). This data demonstrates that expansion of the anterior prechordal plate is due to changes in cellular distribution rather than changes in cell number.

Dickopf-1 is an antagonist of Wnt signaling and is expressed in the anterior prechordal plate, and it is a potent regulator of both prechordal plate and anterior head development in *Xenopus* and zebrafish (Kazanskaya et al., 2000; Shinya et al., 2000). In *Astyanax*, *dkk-1* was expressed in a small domain at the midline slightly anterior to or overlapping with the neural plate border at tailbud stage (Figs. 2A, B). The position of these cells overlapped with the most anterior domain of *ndr2* expression (data not shown). In Pachón cavefish, *dkk-1*-expressing-cells were less compact than in surface fish. We performed two-colour *in situ* hybridization for *dkk-1*, *dlx3b* (*distal-less homeobox 3b*) and *shha* to examine the relationship between the neural plate border (marked by *dlx3b*), the midline (by *shha*) and the anterior prechordal plate (by *dkk-1*). In relation to the neural plate border, the most anterior *shha* and *dkk-1* expressing cells in cavefish were placed more anterior than in surface fish. Also, we found that in 62% ($n=21$) of Pachón embryos, *shha* expressing cells were mixed with *dkk-1*-expressing cells. In surface fish, this mixing was only observed in 1 out of 22 embryos (Figs. 2C, D).

Taken together, these data suggest that the cell number in the prechordal plate, as defined by *shha* and *gsc* expression, is the same between the surface fish and Pachón cavefish. However, the cavefish cells are more dispersed and placed more anteriorly, resulting in a wider anterior tip of the prechordal plate. *pax6* expression is reduced in the cavefish at the anterior midline region, and *shha* expression is expanded complementary to the reduction of *pax6*. Fig. 2E summarises the gene expression patterns in the prechordal plate and ANP at tailbud stage (left surface fish, right cavefish).

Inhibition of Nodal signaling rescues some aspects of cavefish eye degeneration

Nodal signaling is required for prechordal plate specification in vertebrates, and *ndr2* has been identified as one of the direct up-stream regulators of *shh* expression at the anterior midline in the zebrafish (Hagos and Dougan, 2007; Müller et al., 2000). To investigate whether Nodal signaling regulates the formation of the prechordal plate and the expansion of *shha* expression in cavefish, we treated embryos with SB431542, a specific inhibitor of TGF- β Type I receptor Alk4/5/7, (Hagos and Dougan, 2007). We treated cavefish embryos with 25 μ M of SB431542 at two different time points. For the early treatment, embryos were treated during prechordal plate specification and migration (from blastula to tailbud stage, 4hrs to 11hrs of post fertilisation). For late treatment, embryos were treated during the time of induction of *shha* expression (from late gastrula to early somitogenesis stage, 8hrs to 15hrs post fertilisation). To understand the effect of nodal inhibition on prechordal plate size we performed *in situ* hybridization for *gsc* and *dkk-1*. After the early treatment, the intensity of *gsc* expression was weaker, with a narrower width of the expression domain, and a diminished expanded anterior expression (arrowheads in Figs. 3A, A'). The late treatment also slightly reduced *gsc* expression especially at the expanded anterior domain, compared with DMSO-treated control embryos (arrowheads in Figs. 3A, A"). The *dkk-1* expression domain was also reduced in both the early and later treatment, and it was not as dispersed as in the control embryos (Figs. 3B-B").

To understand how nodal inhibition affected *shh* expression and ANP patterning, we examined the expression of *shha* and *pax6*. After early treatment, expression of *shha* was diminished at the anterior midline and failed to reach the anterior neural plate border marked by expression of *dlx3b* (14 out of 14, Figs. 3C, C'). The later treatment also slightly reduced the *shha* expression domain, which also did not reach the neural plate border (15 out of 15, Fig. 3C"). Interestingly, after SB treatment, we did not observe a bent (left or right) or a zigzag pattern of *shha* expression, which was often found in cavefish embryos (Fig. 3F). Instead, the expression pattern of the treated embryos became a straight line, similar to what was found in the surface fish.

After the early treatment, the gap between the left and right domain of *pax6* expression was narrower, and the most anterior domain of *pax6* expression had increased and filled the gap (Figs. 3D, D', E, E'). After the later treatment, *pax6*

expression also increased slightly at the anterior gap and more rostral domains (arrows Figs. 3D, D", E, E"). Two-colour *in situ* showed that the increased expression of *pax6* corresponds to the reduction of *shha* at the anterior midline (Figs. 3F, F'). The expression domains in the presumptive lens were also slightly bigger in the treated fish (arrowheads in Figs. 3E-E").

These data suggest down-regulation of Nodal signaling in the cavefish, reduced expansion of the prechordal plate as marked by *gsc*, *dkk-1* and *shha*, and extended eye and lens fields in the ANP as marked by *pax6*.

To investigate whether reduction of Nodal signaling can rescue eye degeneration in cavefish, we measured the size of optic cup and lens, as well as examined lens apoptosis by acridine orange staining in 48hrs larvae. After the early SB treatment, the treated larvae had a 20% larger total lens area (Fig. 3H) and 13% larger optic cup area, as measured from lateral view (n=44, Fig. 3I). After the later treatment, some of the larvae had slightly enlarged lens and optic cup, but the size difference was not significant between the DMSO and SB-treated embryos (n=33, Figs. 3H, I). This difference between early and later treatments correlated with the level of reduction of *shha* and enhancement of *pax6* expression at the anterior midline described above. For lens degeneration, apoptosis was detected in the lens of 48hrs larvae after both treatment regimens (n=19, Figs. 3J, J'). Later in development, eye degeneration in SB treated embryos was similar to control embryos.

To investigate whether Nodal signaling is essential for eye degeneration during somitogenesis, we treated cavefish embryos with SB from early to late somitogenesis stage (11 to 24 hours post fertilization). Treated embryos were not significantly different from the controls in aspects of lens size, optic cup size or lens apoptosis (n=28, Figs. 3H, I). These data suggest that down-regulation of Nodal signaling before somitogenesis could rescue some aspects of cavefish eye degeneration (increasing the size of the lens and optic cup), but it could not prevent apoptosis in the lens and eye degeneration later in development.

Up-regulation of Nodal signaling reduces eye size in surface fish.

To investigate whether up-regulation of Nodal signaling can enhance anterior midline signaling and initiate eye degeneration in surface fish, we injected *smad2CA* mRNA into 2-cell stage surface fish embryos. Smad2CA is a constitutively active form of Smad2,

which is a downstream effector of the Nodal signaling pathway. In zebrafish, over-expression of *smad2CA* in the early embryo enhanced Nodal signaling, resulting in increased *shha* expression (Maurus and Harris, 2009; Müller et al., 2000). After microinjection of 75pg of *smad2CA* mRNA, the expression of *gsc* and *shha* showed slightly expanded domains at the anterior midline of surface fish embryos (arrowheads in Figs. 4A, A', B, B'). Embryos injected with 150pg of *smad2CA* mRNA showed a widely expanded expression of *gsc* and *shha* at the anterior midline (arrowheads in Figs. 4A, A'', B, B''). Interestingly, the *shha* expression domain often expanded to the left or right similar to what was often observed in the cavefish, but never in surface fish embryos. In 50% of injected embryos, the anterior *shha* expression area reached the neural plate border marked by *dlx3b* (n=18, Fig. 4B''). The *pax6* expression domain was also reduced in the ANP, and the gap between left and right domains was slightly wider than in control embryos (Figs. 4C-C''). The *pax6* expression domains in the presumptive lens epithelium were reduced at the anterior midline, and staining intensity was weaker compared to control *nGFP* mRNA injected embryos (arrowheads Figs. 4D-D''). These data suggest that up-regulation of Nodal signaling enhanced anterior expansion of the prechordal plate and reduced *pax6* expression at anterior midline.

We also examined the size of optic cup and lens in 48hrs surface fish embryos after up-regulation of Nodal signaling. After injection of 75pg of *smad2CA* mRNA into surface fish embryos, the lens and optic cup area were slightly smaller (19% in lens and 15% in optic cup area, n=27, Figs. 4G, H). Increasing the amount of mRNA to 150pg did not decrease the size of the lens and optic cup further, but only reduced the variability of the size reduction. *Smad2CA* injected larvae did not show any apoptotic cells in the lens after staining with acridine orange (data not shown). We also did not detect any eye or lens degeneration at later stages. These data suggest that up-regulation of Nodal signaling could impact on anterior midline signaling, reducing *pax6* expression in the ANP, and reducing lens and optic cup size. However, it cannot initiate eye degeneration in the surface fish.

Hypothalamus and optic stalk are reduced after the inhibition of Nodal signaling in cavefish

It has been reported that cavefish embryos have a larger hypothalamus and optic stalks than surface fish (Menuet et al., 2007; Yamamoto et al., 2004). Midline expansion and

changes in Nodal signaling could be responsible for these differences. To test this, we examined expression patterns of marker genes for the hypothalamus and optic stalks (*nkx2.4b* (NK2 homeobox 4b) and *pax2*, respectively) after inhibition of Nodal signaling in cavefish. The expression domain of *nkx2.4b* was significantly reduced at the 10-somite stage, especially in the anterior domain of the hypothalamus region (arrows in Figs. 5A, A'). At the 15-somite stage, the optic vesicle of the treated embryos was located more anteriorly than untreated embryos. The anterior hypothalamus was also smaller in treated embryos (black-arrows in Figs. 5B, B'). The expression domain of *pax2* in the optic vesicle was also reduced (Figs. 5B, B'). In 24hrs embryos, *pax2* expression in the optic stalk was slightly reduced (arrows, Figs. 5C, C') in SB treated embryo. However, *pax2* expression in the midbrain-hindbrain boundary was not affected (arrowheads, Figs. 5B, B'). These results suggest that Nodal signaling is associated with cavefish features such as a larger hypothalamus and robust optic stalks.

Levels of *shh* expression at the anterior midline control the tissue ratio between the neural retina and optic stalk in zebrafish and cavefish (Macdonald et al., 1995; Yamamoto et al., 2004). We have shown that the level of Nodal signaling during embryonic development could control the expression of *shha* and *pax6* in the ANP, which also affected eye size. However, it is still unclear how changes in *pax6* expression in the anterior midline affect the ratio between the retina and optic stalk in cavefish. To understand this, we examined the cell fate of the anterior midline of the ANP using Dil staining. Midline cells were labelled during tailbud stage using Dil, and the location of the labelled cells was examined at 24 hours post-fertilisation (hpf). Figs. 5D and E showed Dil labelled cells at tailbud stage of Pachón cavefish just after the labelling. Figs. 5F and G showed the Dil labelled cells in the surface fish retina and cavefish optic stalk at 24 hpf, respectively.

Lineage tracing showed the area where the anterior gap of *pax6* expression mainly contributed to the optic stalk and the retina in both morphs. However, in cavefish, positions within the anterior middle gap were more likely to contribute to the optic stalk than in surface fish (Fig. 5H). Overall, in Pachón cavefish larvae, only 29.5% of Dil labelled cells were found in the eyecup, and 35.8% of the labelled cells were found in the optic stalk (n=47). In surface fish larvae 70.2% of the labelled cells were found in the eyecup where only 11.7% were found in the optic stalk (n=54). After early SB treatment (25uM for 4 to 11hpf) in cavefish larvae, the probability of optic stalk contribution in the anterior midline cells was decreased to surface fish levels: only 13.5% of the labelled

cells were found in the optic stalk, and 68.4% of the labelled cells were found in the eyecup (n=22). Interestingly, 30.2% of Dil labelled cells were found in cavefish brain, but after the treatment, this decreased to 15%. The Dil labelled cells in the brain were mostly located in the forebrain (telencephalon and hypothalamus). These data confirmed that cells in the anterior gap of *pax6* expression were more likely to differentiate into non-retinal tissues (optic stalk and forebrain) than into retina in cavefish. Decreasing the anterior gap by Nodal inhibition could lead to a reduction of cell numbers in the non-retinal tissues and an increase in the volume of the neural retina in the treated cavefish embryos.

Changing Spemann's organiser distribution in cavefish

We have shown that inhibition of Nodal signaling can reduce anterior midline signaling, thereby rescuing the size of the optic cup and lens in cavefish embryos. The most effective period of inhibition is during blastula and gastrula stages, when the specification and migration of the prechordal plate occur in Spemann's organiser (Chen and Schier, 2002; Dougan et al., 2003; Gritsman et al., 2000; Hagos and Dougan, 2007). This suggests that the strength of Nodal signaling may differ between surface fish and cavefish in the blastula and gastrula stages, affecting prechordal plate behaviour and distribution. To examine this, we compared expression levels of two Nodal-related genes, *ndr1* and *ndr2* at the shield stage by quantitative PCR. We also investigated expression levels of *gsc*, which has a crucial role for prechordal plate formation and behaviour (Niehrs et al., 1993; Ulmer et al., 2017). We used the Ribosomal protein L13a (*rpl13a*) gene as a reference gene which was similarly expressed in Pachón and Surface fish. We found that *ndr2* expression was slightly increased in cavefish, but the difference is not statistically significant (Fig. 6G, surface fish: 1.36 (n=5), Pachón: 1.57 (n=6), t-test $p > 0.05$). Interestingly, *ndr1* expression was two times higher in cavefish embryos when compared to surface fish (Fig. 6G, surface fish: 2.48 (n=5), Pachón: 6.17 (n=6), t-test $p < 0.01$). In addition, *gsc* expression was almost six times higher in cavefish compared to surface fish (Fig. 6G, surface fish: 4.86 (n=5), Pachón: 28.22 (n=6), t-test $p < 0.001$). These data suggest that Nodal signaling, particularly Ndr1, is enhanced in cavefish at shield stage and this may induce more *gsc* expression in the cavefish embryo.

Specification of prechordal plate occurs in Spemann's organiser during gastrulation. To understand whether increasing *ndr1* and *gsc* expression have an impact

on presumptive prechordal plate cells in the cavefish, we compared the distribution and cell number of the presumptive prechordal plate cells in Spemann's organiser between surface fish and cavefish by using the marker genes *gsc* and *ndr2*. In surface fish embryos, *gsc* and *ndr2* were expressed at the embryonic shield similarly to zebrafish embryos. In Pachón cavefish, these genes were also expressed at the shield stage, however, the expression domain is laterally narrower along the mediolateral axis and wider along the animal-vegetal axis when compared to surface fish embryos (arrowheads, Figs. 6A-D", surface fish; *gsc* (n=15), *ndr2* (n=13), Pachón; *gsc* (n=17), *ndr2* (n=13)). Interestingly, the germ ring was thicker in cavefish than surface fish embryos (arrows, Figs. 6A"-D"). Fig. 6E shows a closed-up dorsal view of *gsc* expression at 40% epiboly and shield stage. In surface fish, *gsc* was expressed in only 3-4 tiers of cells close to the bottom edge of the germ rings at the 40% epiboly stage. However, in cavefish, *gsc* was expressed in 6-7 tiers of cells from the bottom edge. At shield stage, *gsc* was expressed in 7-10 tiers of cells in surface fish embryos, but in cavefish, 10-12 tiers of cells expressed *gsc* in the embryonic shield. Other marker genes for Spemann's organiser, *chordin* and *foxa2* also showed a narrower expression along the mediolateral axis and wider along the animal-vegetal axis in the cavefish when compared to surface fish embryos (data not shown). We also compared the numbers of *gsc*-expressing cells at shield stage between surface fish and cavefish. The number of *gsc*-expressing cells in the cavefish was fewer than that in surface fish embryos, but the difference was not statistically significant (Surface 181 ± 30 n=5; Pachón 169 ± 23 n=6, t-test $p > 0.05$, Fig. 6F). In zebrafish, a mediolaterally narrower Spemann's organiser leads to the formation of a small anterior neural plate (ANP) in the gastrula and formation of a small forehead later in development (Bielen and Houart, 2012; Kudoh et al., 2004; Stewart and Gerhart, 1990). To investigate whether the cavefish has a small ANP, we measured the ANP length (*dlx3-pax2*) and divided by body length (*dlx3-tailbud*) to normalize the embryonic size differences at tailbud embryos. In surface fish, the ANP length is $33.3 \pm 2.2\%$ of the body length (n=8), but in cavefish, the ANP length was only $30.4 \pm 1.8\%$ (n=10, t-test $p < 0.01$). This suggested that cavefish have a smaller ANP than surface fish.

These data suggested that the cell distribution within the Spemann's organiser has been modified during the cavefish evolution and could account for the expanded anterior prechordal plate associated with the smaller ANP. These modifications of early patterning could lead to the formation of a small lens and optic cup in the cavefish.

Discussion

In this study, we have shown that 1) The anterior prechordal plate was expanded in cavefish tailbud embryos and that this expansion matched the anterior reduction of *pax6* expression. 2) This anterior expansion was due to altered cellular distribution (more cells in the anterior, but fewer cells in the posterior prechordal plate) instead of increased total numbers of cells. 3) Down-regulation of Nodal signaling in cavefish embryos caused a reduction of the anterior expansion and rescued expression of *pax6* at the anterior midline. This led to the enlargement of the optic cup and lens in 48hr embryos, but it did not stop lens and eye degeneration at later stages. 4) Up-regulation of Nodal signaling in surface fish embryos expanded the anterior prechordal plate and reduced the anterior expression of *pax6* reminiscent of cavefish embryos. It also reduced the optic cup and lens in surface fish embryos. 5) Inhibition of Nodal signaling in cavefish embryos resulted in diminished cavefish features, including robust optic stalks and an enhanced hypothalamus. Fate-mapping experiments suggested that the wider anterior gap of *pax6* expression could be associated with the enhancement of non-retinal tissues, optic stalks and hypothalamus at the expense of the neural retina in the cavefish. 6) Quantitative PCR suggested that Nodal signaling was enhanced in the cavefish early gastrulae, which may have led to the increased expression of *gsc* in the presumptive prechordal plate cells. Numbers of presumptive prechordal plate cells was not significantly different between the surface fish and cavefish. However, the distribution of the cells in Spemann's organiser was different between the two morphs. The unique cellular distribution at the early gastrula stage could contribute to the expansion of the anterior prechordal plate and eye degeneration in the cavefish.

Midline signaling and eye degeneration

In the cavefish, the expansion of the anterior prechordal plate is associated with a wider midline gap of *pax6* expression at the ANP, which is negatively correlated with the size of the optic cup and lens vesicle. In *Xenopus*, medaka and zebrafish embryos, *pax6* expression has a similar expression pattern in the ANP, and Nodal, Shh, and Bone morphogenic proteins (BMPs) are expressed in the prechordal plate located underneath the midline gap (Andreazzoli et al., 1999; Loosli et al., 1998; Placzek and Briscoe, 2005). These signaling molecules may suppress the expression of *pax6* at the midline directly

or indirectly. In zebrafish, Nodal null mutants lose *shh* expression in the prechordal plate and fail to form the midline gap in the ANP. In these embryos, eyes are fused anteriorly and form a cyclopic phenotype similar to a *shh* null mutant (Ekker et al., 1995; Hatta et al., 1994). We showed that both *ndr2* and *shha* were expressed in the prechordal plate and that Nodal signaling controls the expansion of *shha* expression in the prechordal plate by manipulating nodal signaling (Figs. 3 and 4).

Other lines of evidence support that the Nodal and Hedgehog signaling can inhibit *pax6* expression. For example, in the spinal cord, Shh can inhibit *pax6* expression indirectly through induction of *Nkx2.2*, which is a homeobox-containing transcription factor (Briscoe et al., 2000, 1999; Lek et al., 2010; Muhr et al., 2001). Similarly, homologous *nkx2.2* genes, *nkx2.1* and *nkx2.4b* (former name is *Nk2.1a*) are also induced by Nodal and Shh and antagonize the expression of *pax6* in the telencephalon and diencephalon in *Xenopus*, mouse, chicken and zebrafish embryos (Manoli and Driever, 2014; Marín et al., 2002; Pera and Kessel, 1997; Sussel et al., 1999; van den Akker et al., 2008). In zebrafish and *Astyanax*, *nkx2.1*, *2.2* and *2.4b* are expressed in the anterior midline of the ANP, positioned just above the prechordal plate at the tailbud stage. In cavefish embryos, all of the above *nkx2* genes are laterally expanded, and reducing Shh signaling by a specific chemical inhibitor, cyclopamine, prevents the expanded expression (Menuet et al., 2007; Yamamoto et al., 2009). Conversely, enhancement of Shh signaling by injecting its mRNA expanded *nkx2.4b* expression in the ANP (Yamamoto et al., 2009). BMPs are also expressed in the prechordal plate, such as *bmp4* and *bmp7* in zebrafish and *Astyanax*, and have an important role in increasing the gap in *pax6* expression (Hinaux et al., 2016; Pottin et al., 2011; Schmid et al., 2000). In chicken embryos, both *bmp7* and *shh* are expressed in prechordal mesoderm and induces *nkx2.1* expression in ventral midline cells in the forebrain (Dale et al., 1997). BMPs could therefore cooperate with Nodal and Shh to induce expanded expression of *Nkx2* genes in the anterior neural plate of cavefish. These findings indicate that the wider gap of *pax6* expression in cavefish could be explained by the expanded expression of *nkx2.1*, *2.2* and *2.4b* genes suppressing the expression of *pax6* at the anterior midline.

Our fate-mapping experiment suggested that cells in the anterior midline gap of *pax6* likely contribute to the optic stalk or forebrain. These data are consistent with other midline fate maps (Pottin et al., 2011; Varga et al., 1999). However, these fate-mapping experiments suggested that the non-retinal fated (optic stalk or forebrain) and retinal

fated cells tend to mingle together and that there is no clear border between them at the end of gastrulation. This indicates that the fates are not completely determined at the neural plate stage and that the fate would be refined during the dynamic morphogenetic movements of optic vesicle evagination (Hernandez-Bejarano et al., 2015; Ivanovitch et al., 2013). Indeed, the signaling molecules Shh and FGF have essential roles in the forebrain for patterning the optic vesicle (Cardozo et al., 2014; Hernandez-Bejarano et al., 2015; Lupo et al., 2005; Picker and Brand, 2005). During early somitogenesis stage, the optic vesicles bud out from the neural tube with cells in the anterior part of the optic vesicle expressing both *pax2* and *vax1*, and becoming the optic stalk later in development. The posterior part of the optic vesicles expresses *pax6*, and these cells then become the neural retina (Ekker et al., 1995; Macdonald et al., 1995; Schwarz et al., 2000). Shh signaling from the ventral diencephalon induces *pax2* and *vax1* in the anterior optic vesicle, and these genes antagonize *pax6* expression in the posterior optic vesicle (Cardozo et al., 2014; Lee et al., 2008; Sanek et al., 2009; Schwarz et al., 2000; Take-uchi, 2003). In cavefish, *shha* expression in the forebrain is laterally expanded during the somitogenesis stage and the expansion is associated with extended expression of *pax2* and *vax1* into the posterior optic vesicle, which reduced expression of *pax6* leading to the formation of robust optic stalks and smaller optic cups (Yamamoto et al., 2004).

The formation of robust optic stalks in the cavefish could be controlled by two sequential events: 1) enhanced expression of both Nodal and Shha signaling at the end of the gastrula, which suppresses *pax6* expression in the anterior midline; and 2) the expanded expression of *shha* in the diencephalon during somitogenesis, which could induce extended expression of *pax2* and *vax1* in the anterior optic vesicle to form robust optic stalks and reducing the size of optic cup (Figs. 7).

FGF signaling has also been shown to play an important role for optic cup formation in *Astyanax* (Pottin et al., 2011). At the early somitogenesis stage, *fgf8* is expressed two hours earlier in the cavefish telencephalon than in the surface fish. Inhibition of FGF signaling in cavefish embryos, during gastrulation and early somitogenesis, reduces the enhanced *shha* expression in the hypothalamus and increases the size of the optic cup at later stages. Furthermore, inhibition of Shh signaling between late gastrula and early somitogenesis suppressed the early *fgf8* expression in the cavefish telencephalon. These data suggest that both Shh and FGF signaling have a reciprocal interaction and both have important roles for optic cup

formation. However, it is not clear whether the FGF signaling could have an impact on the anterior expansion of the prechordal plate. FGF signaling has a pivotal role for cellular motility during gastrulation in mouse and *Xenopus* (Chung et al., 2005; Sun et al., 1999) and controls the anterior migration of prechordal plate cells in Medaka fish (Shimada et al., 2007). It would be interesting to investigate whether FGF has a vital role in cellular migration and the anterior expansion of prechordal plate in the cavefish.

The reduction in the size of lens vesicles in the cavefish is also linked to the expanded anterior prechordal plate, which could reduce *pax6* expression in the lens placode. Nodal and Shh, acting as signaling molecules in the prechordal plate, may have an important role to play. Expression patterns of *bmp4* in the prechordal plate are also modified in cavefish, and ectopic enhancements of BMP signaling in the tailbud embryos increased the lens vesicles in cavefish (Hinaux et al., 2016). This suggests that BMP signaling in embryos could have a role in the formation of the small lens vesicle in cavefish together with Nodal and Shh. It is interesting to note that at the somitogenesis stage, *pax6* expression in the optic vesicle has a pivotal role in inducing a lens vesicle in mouse and chicken embryos (Canto-Soler and Adler, 2006; Klimova and Kozmik, 2014). Therefore reduction of Pax6 in the posterior optic vesicle might also contribute to the formation of the small lens vesicles in the cavefish.

We showed that inhibition of Nodal signaling in cavefish could rescue the formation of the optic cups and lens vesicles. However, the inhibition could not stop further eye degeneration. Cells in the lens vesicles underwent apoptosis and degenerated later in development. This indicates that the reduction of Nodal signaling itself is not sufficient to stop eye degeneration. Indeed, the rescued optic cups and lens vesicles in cavefish were still smaller than those in surface fish. Inability to rescue the eye degeneration completely could be related to the size of the ANP, as the treated embryos still displayed a reduced ANP. A small ANP may lead to the formation of optic cups and lenses of insufficient size to prevent the eye degeneration happening in the cavefish. Similarly, the enhancement of nodal signaling could reduce the size of optic cups and lens vesicles in surface fish embryos but failed to induce apoptosis in the lens and subsequent eye degeneration. However, enhancement of Shh signaling in the surface fish embryos induced apoptosis in the lens that lead to eye degeneration at later development (Yamamoto et al., 2004). This suggests that upregulation of Shh by enhancement of Nodal signaling alone is not sufficient to induce eye degeneration and other signaling molecules. Indeed, FGF and BMP may be required to modify the midline

patterning in the surface fish embryo further to induce the eye degeneration. Indeed, QTL analysis showed 12 loci in the cavefish genome that could have an important role for eye degeneration (Protas et al., 2008), suggesting that multiple factors are involved in inducing the eye degeneration in cavefish.

Mechanisms of anterior expansion of prechordal plate in cavefish

We have shown that modified midline signaling in cavefish plays a central role in many cavefish phenotypes, such as reduction of both the optic cups and lens vesicles and enlargement of the optic stalks. The expansion of the anterior prechordal plate can be seen as the first step of cavefish eye degeneration as it controls midline signaling. In zebrafish, presumptive prechordal plate cells are induced by Nodal signaling in the blastula, and these cells are located in Spemann's organiser in gastrula (Chen and Schier, 2002; Gritsman et al., 2000; Hagos and Dougan, 2007; Schier, 2009; Tian et al., 2003). During gastrulation, the prechordal plate cells migrate toward the animal pole as a highly cohesive group controlled by Wnt, PDGF and Nodal signalling (Tada and Heisenberg, 2012). At the end of gastrulation, the anterior prechordal plate cells stop migrating after reaching the anterior border between the neural and non-neural ectoderm (Tada and Heisenberg, 2012; Tada and Kai, 2012). In *Astyanax* embryos, prechordal plate cells are also induced at blastula stage and are located in Spemann's organiser as indicated by *gsc* expression. Our study provides evidence that prechordal plate cell distribution is different between surface fish and cavefish, with more cells located anteriorly in the cavefish.

Two potential mechanisms could enhance the anterior midline expansion in cavefish: increased cell movement towards the anterior and smaller anterior neural plate. In surface fish, the distribution of prechordal plate cells along the anterior-posterior axis is uniform, according to the expression patterns of *ndr2*, *shha* and *gsc* (Figs. 1-3). Whereas In cavefish, there are more cells in the anterior prechordal plate than in the posterior part. The widest point of the anterior prechordal plate in cavefish is nine cells wide, but the widest point in the surface fish is only six cells wide (Yamamoto et al., 2004). However, the total number of prechordal plate cells is not significantly different (*shha* and *gsc* expressing cells), so the increase in anterior cell numbers is likely due to enhanced cellular movement in this direction. In zebrafish, Nodal signaling regulates the motility of endodermal cells through activating Rac1, a Rho-family small GTPases, and

inhibition of Nodal signaling during gastrulation leads to slower migration (Woo et al., 2012). In surface fish, enhancement of Nodal signaling, by *Smad2CA* mRNA injection, resulted in more cells being distributed in the anterior prechordal plate with the most anterior cells reaching the border between the non-neural and neural ectoderm. This usually does not occur in surface fish tailbud embryos (Fig. 4). Inhibition of Nodal signaling in cavefish gastrula prevented the prechordal plate cells from reaching the anterior neural plate border, which typically occurs in cavefish embryos (Fig. 3). Furthermore, our RT-PCR data suggested that *nodal* transcription was higher in cavefish gastrulae than surface fish gastrulae. Therefore, this enhanced Nodal signaling may up-regulate cellular motility and cause anterior expansion of the prechordal plate in cavefish embryos. Moreover, expression of *gsc* is strongly up-regulated in the cavefish gastrula (Fig. 6G) and Goosecoid is known to have a vital role in cellular motility of the prechordal plate and is also induced by Nodal signaling (Gritsman et al., 2000; Jones et al., 1995; Luu et al., 2008; Niehrs et al., 1993; Sampath et al., 1997; Toyama et al., 1995). For example, up-regulation of *gsc* enhanced the cellular migration in the *Xenopus* gastrulae (Niehrs et al., 1993). In our study, microinjection of *gsc* mRNA into dorsal blastomeres at the 32cell stage led to *gsc* enhanced cells to move more anteriorly than cells that did not receive *gsc* mRNA. This also changed the cell fate of caudal mesoderm such as the notochord and somite into cranial endo-mesoderm (head mesenchyme, prechordal plate and pharyngeal endoderm). Interestingly, we could not detect significantly increased *ndr2* expression. However, although increased *ndr1* expression may be sufficient to increase *gsc* expression, time of exposure to Nodal signalling, not just the strength, is also crucial for induction of *gsc* (Boxtel et al., 2015). Further experiments are necessary to understand the relationship between *ndr1*, *ndr2* and *gsc* in the cavefish and to test the hypothesis that higher expression of *ndr1* and *gsc* leads to increased anterior movement of prechordal plate cells leading to anterior prechordal plate expansion in cavefish embryos.

The second possible scenario that could affect the shape of the prechordal plate is the smaller anterior neural plate (ANP) observed in cavefish embryos. About half of cavefish embryos showed a unique pattern of the prechordal plate, which exhibits a zigzagged or bend pattern (Figs. 1D and 3F). Cavefish tailbuds embryos have a slightly shortened ANP (shorter along the anterior-posterior axis) when compared to the surface fish. Shortened ANP means there is less space for cell movement, which may result in the accumulation of cells at the anterior tip. As more posterior prechordal plate cells

continue to move anteriorly, anterior cells already present could impede their movement and causing cells to move laterally, resulting in a bend or zigzagged expression pattern. The anterior prechordal plate cells (*dkk-1* expressing cells) were shown to intermingle with posterior *shha* expressing cells (Fig. 2) suggesting that posterior cells are indeed encroaching on the anterior territory. A similar intermingling phenomenon was also reported between *bmp4* and *shha* expressing cells in the cavefish anterior prechordal plate (Hinaux et al., 2016).

In summary, the enhanced cellular motility and smaller anterior neural plate may coordinate the anterior expansion of the cavefish prechordal plate. Further investigation is needed to understand how this contribution to expansion is achieved.

Spemann's Organiser and prechordal plate development

Enhancement of cellular motility in the gastrula and formation of a smaller anterior neural plate at the tailbud stage suggest early developmental processes were modified in cavefish embryos. This early change could originate from Spemann's organiser, which has an important role in establishing the border between non-neural and neural-ectoderm by secreting antagonists of BMP signaling. In zebrafish, a reduced Spemann's organiser leads to the development of a smaller ANP at the tailbud stage (Bielen and Houart, 2012; Kudoh et al., 2004; Stewart and Gerhart, 1990). Our observation of differences in Spemann's organiser between cavefish and surface fish add support to this hypothesis. The cavefish Spemann's organiser (marked by *gsc* and *ndr2*) is mediolaterally narrower and wider towards the animal pole at shield stage (Fig. 6). Before initiation of gastrulation, at the 40% epiboly stage, the *gsc* expression domain is also laterally narrower in cavefish embryos, suggesting that cavefish embryos could be ventralised. However, the number of cells expressing *gsc* in the Spemann's organiser is not significantly different between surface fish and cavefish. Wider expression of *gsc* along an animal-vegetal axis in cavefish blastula suggests Nodal signaling is enhanced in the blastula. It has been shown that enhancement of Nodal signaling in the zebrafish blastula leads to a wider germ ring at gastrula stage (Feldman et al., 2002), which is also observed in the cavefish gastrula (Fig. 6). A wider germ ring in the cavefish, as a result of enhanced Nodal signaling, could affect the shape of the organiser. Cells within the Spemann's organiser are patterned by complex interacting morphogenetic gradients.

Differences in cellular arrangement could lead to cell groups experiencing these morphogens differently, leading to patterning differences.

A precise series of molecular events are necessary for the formation of Spemann's organiser, which include localisation of maternal factors in the yolk, β -catenin accumulation in the nucleus, and expression of Nodal-related signals in the germ ring (Jones et al., 1995; Schier, 2009; Tuazon and Mullins, 2015). Interestingly, cavefish have slightly bigger yolk content in the egg (Hinaux et al., 2011; Hüppop and Wilkens, 1991). The increased yolk content may have some influence on the distribution of maternal factors, which in turn could affect patterning.

Modifying early developmental patterning events can affect a group of related features ensuring that the development and changes in the morphology of these features happen in a coordinated and organised way. In the case of cavefish, expansion of Shh signaling resulted in a reduction of eye size and a corresponding expansion of jaw size. We have shown in this study that this change may be the consequences of changes early in development during the patterning of Spemann's organiser. More careful and intensive research is necessary to understand the mechanism behind the unique shape of cavefish Spemann's organiser and whether it has an impact on the anterior expansion of the prechordal plate and the development of cavefish specific traits, such as enhanced other sensory organs, specialized brain, and enhanced feeding apparatus

Acknowledgements

We would like to thank Prof Leslie Dale, Prof David Whitmore, Dr. Tom Hawkins, and Dr Mathilda Mommersteeg for helpful comments and critical reading of the manuscript. We also thank anonymous reviewers for giving us very thoughtful and useful comments.

Funding

This work was supported by the Biotechnology and Biological Sciences Research Council [BB/C517041/1] and the British Heart Foundation [PG/12/39/29626].

Reference

- Andreazzoli, M., Gestri, G., Angeloni, D., Menna, E., Barsacchi, G., 1999. Role of Xrx1 in *Xenopus* eye and anterior brain development. *Development* 126, 2451–2460.
- Ashery-Padan, R., Gruss, P., 2001. Pax6 lights-up the way for eye development. *Curr. Opin. Cell Biol.* 13, 706–714. [https://doi.org/10.1016/S0955-0674\(00\)00274-X](https://doi.org/10.1016/S0955-0674(00)00274-X)
- Bielen, H., Houart, C., 2012. BMP signaling protects telencephalic fate by repressing eye identity and its Cxcr4-dependent morphogenesis. *Dev. Cell* 23, 812–22. <https://doi.org/10.1016/j.devcel.2012.09.006>
- Boxtel, A.L. Van, Chesebro, J.E., Heliot, C., Ramel, M., Stone, R.K., 2015. Article A Temporal Window for Signal Activation Dictates the Dimensions of a Nodal Signaling Domain Article A Temporal Window for Signal Activation Dictates the Dimensions of a Nodal Signaling Domain. *Dev. Cell* 35, 175–185. <https://doi.org/10.1016/j.devcel.2015.09.014>
- Briscoe, J., Pierani, a, Jessell, T.M., Ericson, J., 2000. A homeodomain protein code specifies progenitor cell identity and neuronal fate in the ventral neural tube. *Cell* 101, 435–445. [https://doi.org/10.1016/S0092-8674\(00\)80853-3](https://doi.org/10.1016/S0092-8674(00)80853-3)
- Briscoe, J., Sussel, L., Serup, P., Hartigan-O'Connor, D., Jessell, T.M., Rubenstein, J.L., Ericson, J., 1999. Homeobox gene Nkx2.2 and specification of neuronal identity by graded Sonic hedgehog signalling [In Process Citation]. *Nature* 398, 622–627. <https://doi.org/10.1038/19315>
- Canto-Soler, M.V., Adler, R., 2006. Optic cup and lens development requires Pax6 expression in the early optic vesicle during a narrow time window. *Dev. Biol.* 294, 119–132. <https://doi.org/10.1016/j.ydbio.2006.02.033>
- Cardozo, M.J., Sánchez-Arrones, L., Sandonis, Á., Sánchez-Camacho, C., Gestri, G., Wilson, S.W., Guerrero, I., Bovolenta, P., 2014. Cdon acts as a Hedgehog decoy receptor during proximal-distal patterning of the optic vesicle. *Nat. Commun.* 5. <https://doi.org/10.1038/ncomms5272>
- Chen, Y., Schier, A.F., 2002. Lefty proteins are long-range inhibitors of Squint-mediated Nodal signaling. *Curr. Biol.* 12, 2124–2128. [https://doi.org/10.1016/S0960-9822\(02\)01362-3](https://doi.org/10.1016/S0960-9822(02)01362-3)
- Chung, H.A., Hyodo-Miura, J., Nagamune, T., Ueno, N., 2005. FGF signal regulates gastrulation cell movements and morphology through its target NRH. *Dev. Biol.* 282, 95–110. <https://doi.org/10.1016/j.ydbio.2005.02.030>
- Dale, J.K., Vesque, C., Lints, T.J., Sampath, T.K., Furley, A., Dodd, J., Placzek, M.,

1997. Cooperation of BMP7 and SHH in the induction of forebrain ventral midline cells by prechordal mesoderm. *Cell* 90, 257–269. [https://doi.org/10.1016/S0092-8674\(00\)80334-7](https://doi.org/10.1016/S0092-8674(00)80334-7)
- Dougan, S.T., 2003. The role of the zebrafish nodal-related genes *squint* and *cyclops* in patterning of mesendoderm. *Development* 130, 1837–1851. <https://doi.org/10.1242/dev.00400>
- Dougan, S.T., Wargha, R.M., Kane, D. a, Schier, A.F., Talbot, W.S., 2003. The role of the zebrafish nodal-related genes *squint* and *cyclops* in patterning of mesendoderm. *Development* 130, 1837–1851. <https://doi.org/10.1242/dev.00400>
- Ekker, S.C., Ungar, A.R., Greenstein, P., von Kessler, D.P., Porter, J.A., Moon, R.T., Beachy, P.A., 1995. Patterning activities of vertebrate hedgehog proteins in the developing eye and brain. *Curr. Biol.* 5, 944–955. [https://doi.org/10.1016/S0960-9822\(95\)00185-0](https://doi.org/10.1016/S0960-9822(95)00185-0)
- Feldman, B., Concha, M.L., Saúde, L., Parsons, M.J., Adams, R.J., Wilson, S.W., Stemple, D.L., 2002. Lefty antagonism of *Squint* is essential for normal gastrulation. *Curr. Biol.* 12, 2129–2135. [https://doi.org/10.1016/S0960-9822\(02\)01361-1](https://doi.org/10.1016/S0960-9822(02)01361-1)
- Gehring, W.J., 2005. New perspectives on eye development and the evolution of eyes and photoreceptors. *J. Hered.* 96, 171–84. <https://doi.org/10.1093/jhered/esi027>
- Geng, X., Oliver, G., Geng, X., Oliver, G., 2009. Pathogenesis of holoprosencephaly
Find the latest version : Science in medicine Pathogenesis of holoprosencephaly 119, 1403–1413. <https://doi.org/10.1172/JCI38973.comprised>
- Gritsman, K., Talbot, W.S., Schier, a F., 2000. Nodal signaling patterns the organizer. *Development* 127, 921–932.
- Gross, J.B., Protas, M., Conrad, M., Scheid, P.E., Vidal, O., Jeffery, W.R., Borowsky, R., Tabin, C.J., 2008. Synteny and candidate gene prediction using an anchored linkage map of *Astyanax mexicanus*. *Proc. Natl. Acad. Sci. U. S. A.* 105, 20106–20111. <https://doi.org/10.1073/pnas.0806238105>
- Hagos, E.G., Dougan, S.T., 2007. Time-dependent patterning of the mesoderm and endoderm by Nodal signals in zebrafish. *BMC Dev. Biol.* 7, 1–18. <https://doi.org/10.1186/1471-213X-7-22>
- Hatta, K., Püschel, a W., Kimmel, C.B., 1994. Midline signaling in the primordium of the zebrafish anterior central nervous system. *Proc. Natl. Acad. Sci. U. S. A.* 91, 2061–2065. <https://doi.org/10.1073/pnas.91.6.2061>
- Hecht, M.K., Wallace, B., Wilkens, H., 1988. Evolution and genetics of epigeal and cave

- Astyanax fasciatus (Characidae, Pisces): support for the neutral mutation theory. *Evol. Biol.* 23, 271–367. https://doi.org/10.1007/978-1-4613-1043-3_8
- Hernandez-Bejarano, M., Gestri, G., Spawls, L., Nieto-Lopez, F., Picker, A., Tada, M., Brand, M., Bovolenta, P., Wilson, S.W., Cavodeassi, F., 2015. Opposing Shh and Fgf signals initiate nasotemporal patterning of the retina. *Development* 3933–3942. <https://doi.org/10.1242/dev.125120>
- Hinaux, H., Devos, L., Blin, M., Elipot, Y., Bibliowicz, J., Alié, A., Rétaux, S., 2016. Sensory evolution in blind cavefish is driven by early embryonic events during gastrulation and neurulation. *Development* 143, 4521–4532. <https://doi.org/10.1242/dev.141291>
- Hinaux, H., Pottin, K., Chalhoub, H., Père, S., Elipot, Y., Legendre, L., Rétaux, S., 2011. A Developmental Staging Table for Astyanax mexicanus Surface Fish and Pachon Cavefish. *Zebrafish* 8, 155–165. <https://doi.org/10.1089/zeb.2011.0713>
- Hüppop, K., Wilkens, H., 1991. Bigger eggs in subterranean Astyanax fasciatus. *Zool. Syst. Evol.* 29, 280–288.
- Ivanovitch, K., Cavodeassi, F., Wilson, S.W., 2013. Precocious Acquisition of Neuroepithelial Character in the Eye Field Underlies the Onset of Eye Morphogenesis. *Dev. Cell* 27, 293–305. <https://doi.org/10.1016/j.devcel.2013.09.023>
- Jeffery, W.R., 2008. Emerging model systems in evo-devo: Cavefish and microevolution of development. *Evol. Dev.* 10, 265–272. <https://doi.org/10.1111/j.1525-142X.2008.00235.x>
- Jeffery, W.R., Martasian, D.P., 1998. Evolution of eye regression in the cavefish Astyanax: Apoptosis and the Pax-6 gene. *Am. Zool.* 38, 685–696. <https://doi.org/10.1093/icb/38.4.685>
- Jones, C.M., Kuehn, M.R., Hogan, B.L.M., Smith, J.C., Wright, C.V.E., 1995. Nodal-related signals induce axial mesoderm and dorsalize mesoderm during gastrulation. *Development* 121, 3651–3662.
- Kazanskaya, O., Glinka, A., Niehrs, C., 2000. The role of Xenopus dickkopf1 in prechordal plate specification and neural patterning. *Development* 127, 4981–4992.
- Klimova, L., Kozmik, Z., 2014. Stage-dependent requirement of neuroretinal Pax6 for lens and retina development. *Development* 141, 1292–302. <https://doi.org/10.1242/dev.098822>
- Kudoh, T., Concha, M.L., Houart, C., Dawid, I.B., Wilson, S.W., 2004. Combinatorial Fgf

and Bmp signalling patterns the gastrula ectoderm into prospective neural and epidermal domains. *Development* 131, 3581–3592.

<https://doi.org/10.1242/dev.01227>

- Lee, J., Willer, J.R., Willer, G.B., Smith, K., Gregg, R.G., Gross, J.M., 2008. Zebrafish blowout provides genetic evidence for Patched1-mediated negative regulation of Hedgehog signaling within the proximal optic vesicle of the vertebrate eye. *Dev. Biol.* 319, 10–22. <https://doi.org/10.1016/j.ydbio.2008.03.035>
- Lek, M., Dias, J.M., Marklund, U., Uhde, C.W., Kurdija, S., Lei, Q., Sussel, L., Rubenstein, J.L., Matise, M.P., Arnold, H.-H., Jessell, T.M., Ericson, J., 2010. A homeodomain feedback circuit underlies step-function interpretation of a Shh morphogen gradient during ventral neural patterning. *Development* 137, 4051–4060. <https://doi.org/10.1242/dev.054288>
- Loosli, F., Köster, R.W., Carl, M., Krone, A., Wittbrodt, J., 1998. Six3, a medaka homologue of the *Drosophila* homeobox gene *sine oculis* is expressed in the anterior embryonic shield and the developing eye. *Mech. Dev.* 74, 159–164. [https://doi.org/10.1016/S0925-4773\(98\)00055-0](https://doi.org/10.1016/S0925-4773(98)00055-0)
- Lupo, G., Liu, Y., Qiu, R., Chandraratna, R.A.S., Barsacchi, G., He, R.-Q., Harris, W.A., 2005. Dorsoventral patterning of the *Xenopus* eye: a collaboration of Retinoid, Hedgehog and FGF receptor signaling. *Development* 132, 1737–1748. <https://doi.org/10.1242/dev.01726>
- Luu, O., Nagel, M., Wacker, S., Lemaire, P., Winklbauer, R., 2008. Control of gastrula cell motility by the Goosecoid/Mix.1/ Siamois network: Basic patterns and paradoxical effects. *Dev. Dyn.* 237, 1307–1320. <https://doi.org/10.1002/dvdy.21522>
- Macdonald, R., Barth, K. a, Xu, Q., Holder, N., Mikkola, I., Wilson, S.W., 1995. Midline signalling is required for Pax gene regulation and patterning of the eyes. *Development* 121, 3267–78. [https://doi.org/10.1016/0168-9525\(95\)90453-0](https://doi.org/10.1016/0168-9525(95)90453-0)
- Macdonald, R., Wilson, S.W., 1997. Distribution of Pax6 protein during eye development suggests discrete roles in proliferative and differentiated visual cells. *Dev. Genes Evol.* 206, 363–369. <https://doi.org/10.1007/s004270050065>
- Manoli, M., Driever, W., 2014. Nkx2.1 and Nkx2.4 Genes Function Partially Redundant During Development of the Zebrafish Hypothalamus, Preoptic Region, and Pallidum. *Front. Neuroanat.* 8, 1–16. <https://doi.org/10.3389/fnana.2014.00145>
- Marín, O., Baker, J., Puelles, L., Rubenstein, J.L.R., 2002. Patterning of the basal telencephalon and hypothalamus is essential for guidance of cortical projections.

- Development 129, 761–773. <https://doi.org/11830575>
- Maurus, D., Harris, W.A., 2009. Zic-associated holoprosencephaly: Zebrafish Zic1 controls midline formation and forebrain patterning by regulating Nodal, Hedgehog, and retinoic acid signaling. *Genes Dev.* 23, 1461–1473. <https://doi.org/10.1101/gad.517009>
- Menuet, A., Alunni, A., Joly, J.-S., Jeffery, W.R., Rétaux, S., 2007. Expanded expression of Sonic Hedgehog in *Astyanax* cavefish: multiple consequences on forebrain development and evolution. *Development* 134, 845–855. <https://doi.org/10.1242/dev.02780>
- Muhr, J., Andersson, E., Persson, M., Jessell, T.M., Ericson, J., 2001. Groucho-mediated transcriptional repression establishes progenitor cell pattern and neuronal fate in the ventral neural tube. *Cell* 104, 861–873. [https://doi.org/10.1016/S0092-8674\(01\)00283-5](https://doi.org/10.1016/S0092-8674(01)00283-5)
- Müller, F., Albert, S., Blader, P., Fischer, N., Hallonet, M., Strähle, U., 2000. Direct action of the nodal-related signal cyclops in induction of sonic hedgehog in the ventral midline of the CNS. *Development* 127, 3889–3897.
- Niehrs, C., Keller, R., Cho, K.W.Y., De Robertis, E.M., 1993. The homeobox gene goosecoid controls cell migration in *Xenopus* embryos. *Cell* 72, 491–503. [https://doi.org/10.1016/0092-8674\(93\)90069-3](https://doi.org/10.1016/0092-8674(93)90069-3)
- Nornes, S., Clarkson, M., Mikkola, I., Pedersen, M., Bardsley, A., Martinez, J.P., Krauss, S., Johansen, T., 1998. Zebrafish contains two Pax6 genes involved in eye development. *Mech. Dev.* 77, 185–196. [https://doi.org/10.1016/S0925-4773\(98\)00156-7](https://doi.org/10.1016/S0925-4773(98)00156-7)
- Pera, E.M., Kessel, M., 1997. Patterning of the chick forebrain anlage by the prechordal plate. *Development* 124, 4153–62.
- Picker, A., Brand, M., 2005. Fgf signals from a novel signaling center determine axial patterning of the prospective neural retina. *Development* 132, 4951–4962. <https://doi.org/10.1242/dev.02071>
- Placzek, M., Briscoe, J., 2005. The floor plate: Multiple cells, multiple signals. *Nat. Rev. Neurosci.* 6, 230–240. <https://doi.org/10.1038/nrn1628>
- Pottin, K., Hinaux, H., Rétaux, S., 2011. Restoring eye size in *Astyanax mexicanus* blind cavefish embryos through modulation of the Shh and Fgf8 forebrain organising centres. *Development* 138, 2467–76. <https://doi.org/10.1242/dev.054106>
- Protas, M., Conrad, M., Gross, J.B., Tabin, C., Borowsky, R., 2007. Regressive

- Evolution in the Mexican Cave Tetra, *Astyanax mexicanus*. *Curr. Biol.* 17, 452–454.
<https://doi.org/10.1016/j.cub.2007.01.051>
- Protas, M., Jeffery, W.R., 2012. Evolution and development in cave animals: From fish to crustaceans. *Wiley Interdiscip. Rev. Dev. Biol.* 1, 823–845.
<https://doi.org/10.1002/wdev.61>
- Protas, M., Tabansky, I., Conrad, M., Gross, J.B., Vidal, O., Tabin, C.J., Borowsky, R., 2008. Multi-trait evolution in a cave fish, *Astyanax mexicanus*. *Evol. Dev.* 10, 196–209. <https://doi.org/10.1111/j.1525-142X.2008.00227.x>
- Rebagliati, M.R., Toyama, R., Haffter, P., Dawid, I.B., 1998. Cyclops Encodes a Nodal-Related Factor Involved in Midline Signaling. *Proc. Natl. Acad. Sci. U. S. A.* 95, 9932–9937. <https://doi.org/10.1073/pnas.95.17.9932>
- Rohr, K.B., Barth, K.A., Varga, Z.M., Wilson, S.W., 2001. The Nodal pathway acts upstream of Hedgehog signaling to specify ventral telencephalic identity. *Neuron* 29, 341–351. [https://doi.org/10.1016/S0896-6273\(01\)00210-0](https://doi.org/10.1016/S0896-6273(01)00210-0)
- Sampath, K., Cheng, A.M.S., Frisch, A., Wright, C.V.E., 1997. Functional differences among *Xenopus* nodal-related genes in left-right axis determination. *Development* 3302, 3293–3302.
- Sampath, K., Rubinstein, A.L., Cheng, A.M.S., Liang, J.O., Fekany, K., Sonica-Krezel, L., Korzh, V., Halpern, M.E., Wright, C.V.E., 1998. Induction of the zebrafish ventral brain and floorplate requires cyclops/nodal signalling. *Nature* 395, 185–189.
<https://doi.org/10.1038/26020>
- Sanek, N. a, Taylor, A. a, Nyholm, M.K., Grinblat, Y., 2009. Zebrafish *zic2a* patterns the forebrain through modulation of Hedgehog-activated gene expression. *Development* 136, 3791–3800. <https://doi.org/10.1242/dev.037820>
- Schier, A.F., 2009. Nodal morphogens. *Cold Spring Harb. Perspect. Biol.* 1.
<https://doi.org/10.1101/cshperspect.a003459>
- Schmid, B., Fürthauer, M., Connors, S. a, Trout, J., Thisse, B., Thisse, C., Mullins, M.C., 2000. Equivalent genetic roles for *bmp7/snailhouse* and *bmp2b/swirl* in dorsoventral pattern formation. *Development* 127, 957–967.
- Schulte-Merker, S., Hammerschmidt, M., Beuchle, D., Cho, K.W., De Robertis, E.M., Nüsslein-Volhard, C., 1994. Expression of zebrafish goosecoid and no tail gene products in wild-type and mutant no tail embryos. *Development* 120, 843–852.
- Schwarz, M., Cecconi, F., Bernier, G., Andrejewski, N., Kammandel, B., Wagner, M., Gruss, P., 2000. Spatial specification of mammalian eye territories by reciprocal

- transcriptional repression of Pax2 and Pax6. *Development* 127, 4325–4334.
[https://doi.org/10.1016/0092-8674\(91\)90434-z](https://doi.org/10.1016/0092-8674(91)90434-z)
- Shimada, A., Yabusaki, M., Niwa, H., Yokoi, H., Hatta, K., Kobayashi, D., Takeda, H., 2007. Maternal-zygotic medaka mutants for *fgfr1* reveal its essential role in the migration of the axial mesoderm but not the lateral mesoderm. *Development* 135, 281–290. <https://doi.org/10.1242/dev.011494>
- Shinya, M., Eschbach, C., Clark, M., Lehrach, H., Furutani-Seiki, M., 2000. Zebrafish *Dkk1*, induced by the pre-MBT Wnt signaling, is secreted from the prechordal plate and patterns the anterior neural plate. *Mech. Dev.* 98, 3–17.
[https://doi.org/10.1016/S0925-4773\(00\)00433-0](https://doi.org/10.1016/S0925-4773(00)00433-0)
- Stewart, R.M., Gerhart, J.C., 1990. The anterior extent of dorsal development of the *Xenopus* embryonic axis depends on the quantity of organizer in the late blastula. *Development* 109, 363–372.
- Strickler, A.G., Yamamoto, Y., Jeffery, W.R., 2001. Early and late changes in Pax6 expression accompany eye degeneration during cavefish development. *Dev. Genes Evol.* 211, 138–144. <https://doi.org/10.1007/s004270000123>
- Sun, X., Meyers, E.N., Lewandoski, M., Martin, G.R., 1999. Targeted disruption of *Fgf8* causes failure of cell migration in the gastrulating mouse embryo. *Genes Dev.* 13, 1834–1846. <https://doi.org/10.1101/gad.13.14.1834>
- Sussel, L., Marin, O., Kimura, S., Rubenstein, J.L., 1999. Loss of *Nkx2.1* homeobox gene function results in a ventral to dorsal molecular respecification within the basal telencephalon: evidence for a transformation of the pallidum into the striatum. *Development* 126, 3359–3370. <https://doi.org/10393115>
- Tada, M., Heisenberg, C.-P., 2012. Convergent extension: using collective cell migration and cell intercalation to shape embryos. *Development* 139, 3897–3904.
<https://doi.org/10.1242/dev.073007>
- Tada, M., Kai, M., 2012. Planar Cell Polarity in Coordinated and Directed Movements, 1st ed, Current Topics in Developmental Biology. Elsevier Inc.
<https://doi.org/10.1016/B978-0-12-394592-1.00004-1>
- Take-uchi, M., 2003. Hedgehog signalling maintains the optic stalk-retinal interface through the regulation of *Vax* gene activity. *Development* 130, 955–968.
<https://doi.org/10.1242/dev.00305>
- Tian, J., Yam, C., Balasundaram, G., Wang, H., Gore, A., Sampath, K., 2003. A temperature-sensitive mutation in the nodal-related gene *cyclops* reveals that the

- floor plate is induced during gastrulation in zebrafish. *Development* 130, 3331–3342.
<https://doi.org/10.1242/dev.00544>
- Toyama, R., O'Connell, M.L., Wright, C. V, Kuehn, M.R., Dawid, I.B., 1995. Nodal induces ectopic gooseoid and lim1 expression and axis duplication in zebrafish. *Development* 121, 383–91.
- Tuazon, F.B., Mullins, M.C., 2015. Temporally coordinated signals progressively pattern the anteroposterior and dorsoventral body axes. *Semin. Cell Dev. Biol.* 42, 118–133.
<https://doi.org/10.1016/j.semcdb.2015.06.003>
- Ulmer, B., Tingler, M., Kurz, S., Maerker, M., Andre, P., Mönch, D., Campione, M., Deißler, K., Lewandoski, M., Thumberger, T., Schweickert, A., Fainsod, A., Steinbeißer, H., Blum, M., 2017. A novel role of the organizer gene Gooseoid as an inhibitor of Wnt/PCP-mediated convergent extension in *Xenopus* and mouse. *Sci. Rep.* 7, 1–17. <https://doi.org/10.1038/srep43010>
- van den Akker, W.M.R., Brox, A., Puelles, L., Durston, A.J., Medina, L., 2008. Comparative Functional Analysis Provides Evidence for a Crucial Role for the Homeobox Gene *Nkx2.1/Titf-1* in Forebrain Evolution. *J. Comp. Neurol.* 506, 211–223. <https://doi.org/10.1002/cne>
- Varga, Z., Wegner, J., Westerfield, M., 1999. Anterior movement of ventral diencephalic precursors separates the primordial eye field in the neural plate and requires cyclops. *Development* 126, 5533–5546.
- Westerfield, M., 2000. *The Zebrafish Book. A Guide for the Laboratory Use of Zebrafish (Danio rerio)*, 4th Edition, book.
- Wilson, S.W., Houart, C., 2004. Funders Group Early Steps in the Development of the Forebrain. *Dev. Cell* 6, 167–181.
- Woo, S., Housley, M.P., Weiner, O.D., Stainier, D.Y.R., 2012. Nodal signaling regulates endodermal cell motility and actin dynamics via Rac1 and Prex1. *J. Cell Biol.* 198, 941–952. <https://doi.org/10.1083/jcb.201203012>
- Yamamoto, Y., Byerly, M.S., Jackman, W.R., Jeffery, W.R., 2009. Pleiotropic functions of embryonic sonic hedgehog expression link jaw and taste bud amplification with eye loss during cavefish evolution. *Dev. Biol.* 330, 200–211.
<https://doi.org/10.1016/j.ydbio.2009.03.003>
- Yamamoto, Y., Stock, D.W., Jeffery, W.R., 2004. Hedgehog signalling controls eye degeneration in blind cavefish. *Nature* 431, 844–847.
<https://doi.org/10.1038/nature02864>

Figure 1

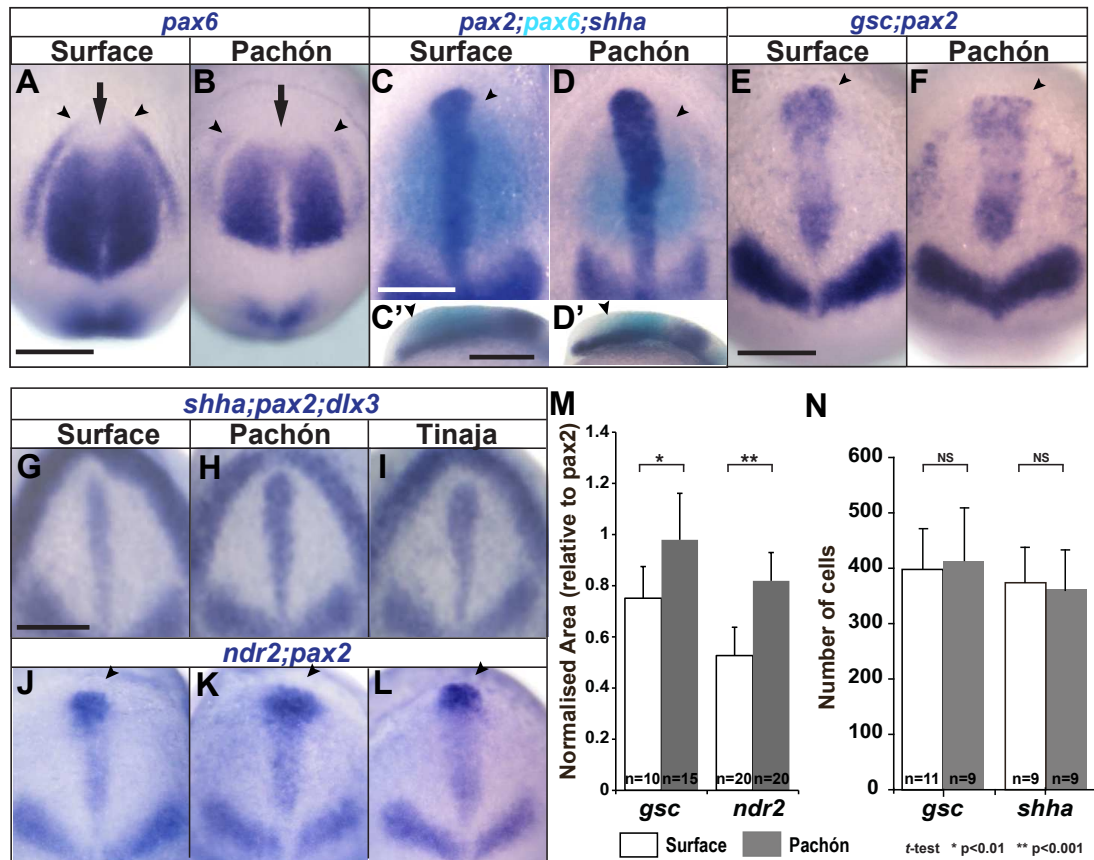


Fig. 1. The anterior prechordal plate is expanded in the cavefish. Its expansion is correlated to expanded expression of *shha* and reduction of *pax6* expression in the ANP. Dorsal view of the ANP in Surface fish (A, C, E, G, J), Pachón cavefish (B, D, F, H, K), and Tinaja cavefish (I, L) and lateral view of the ANP in Surface fish (C') and Pachón cavefish (D'). (A, B, 1-2 somite stage) The overall *pax6* expression domain is smaller in the Pachón cavefish. The expression is reduced in the gap between the left and right domains and especially in the anterior region (arrow). The *pax6* expression in the lens epithelium is also reduced, the gap between the domains is also wider in the cavefish (arrowhead). (C, C', D, D', 1-2 somite stage) The two-colour *in situ* hybridization suggest the reduction in *pax6* (cyan) expression is correlated with the domains of *shha* (dark blue) expanded expression. The anterior edge of *pax6* in the Pachón cavefish is always more posterior than that of *shha* (arrowhead). (E-L, early tailbud stage) Prechordal plate markers, *gsc* (arrowhead, E, F) and *ndr2* (arrowhead, J-L) show the anterior prechordal plate region is also expanded in the cavefish similar to *shha* (G-I).

(M) Quantification of *gsc* and *ndr2* expressing areas shows prechordal plate area in the ANP is larger in the cavefish. (N) The number of *gsc* and *shha* expressing cells is not significantly different between Pachón and surface fish. Scale bars, 250 μm .

Figure 2

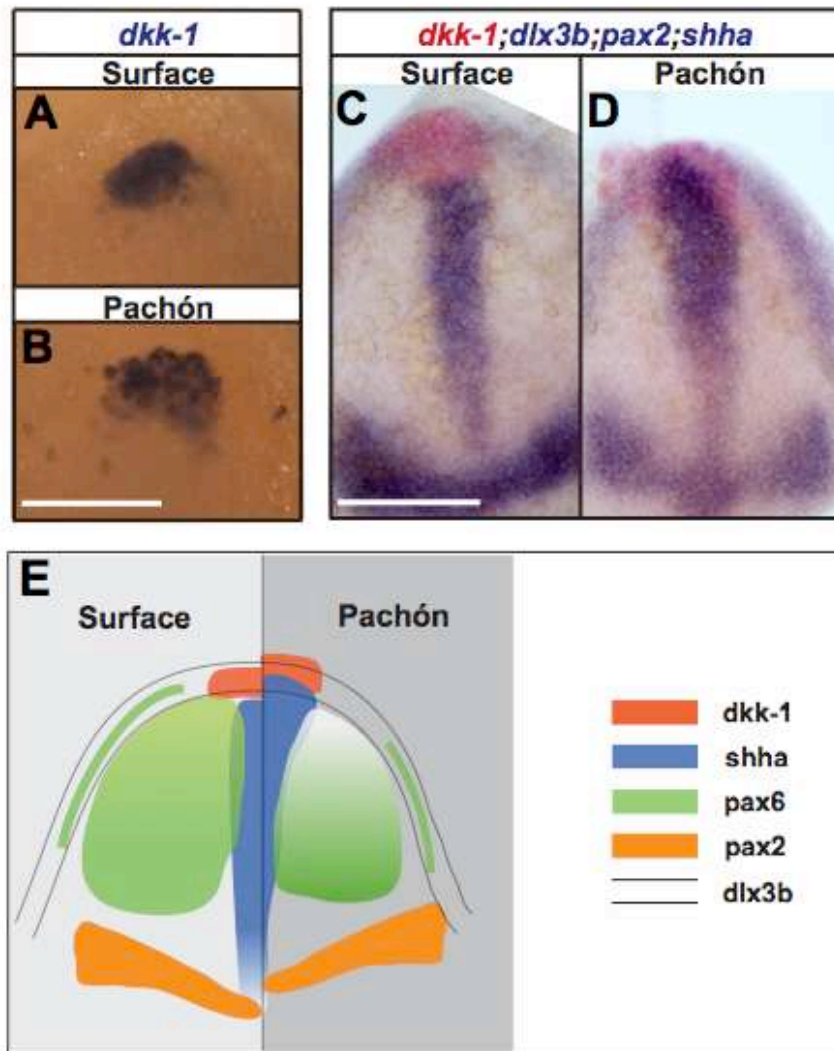


Fig. 2. The relationship between the prechordal plate and ANP suggests the midline cells migrate more anteriorly in the cavefish. Dorsal view of the ANP of Surface (A, C), Pachón (B, D) tailbud stage embryos. To understand the relationship between different regions of the ANP, we performed two-colour *in situ* hybridization with *dkk-1*, *dlx3b*, *pax2*, and *shha* probes. (A, B) The *in situ* hybridization show the *dkk-1* expression domain in the anterior prechordal plate. The expressing cells are more dispersed in the cavefish. (C, D) The *in situ* hybridization shows the tip of *shha* expression domain (dark blue), and *dkk-1* domain (red) are more anterior to the neural plate border *dlx3b* expression (dark blue) in the cavefish. The *shha* expressing cells invade into the *dkk-1* expression domain (red) in the cavefish. (E) Summary of the expression differences in the ANP between surface fish and cavefish. Scale bars, 250 μm .

Figure 3

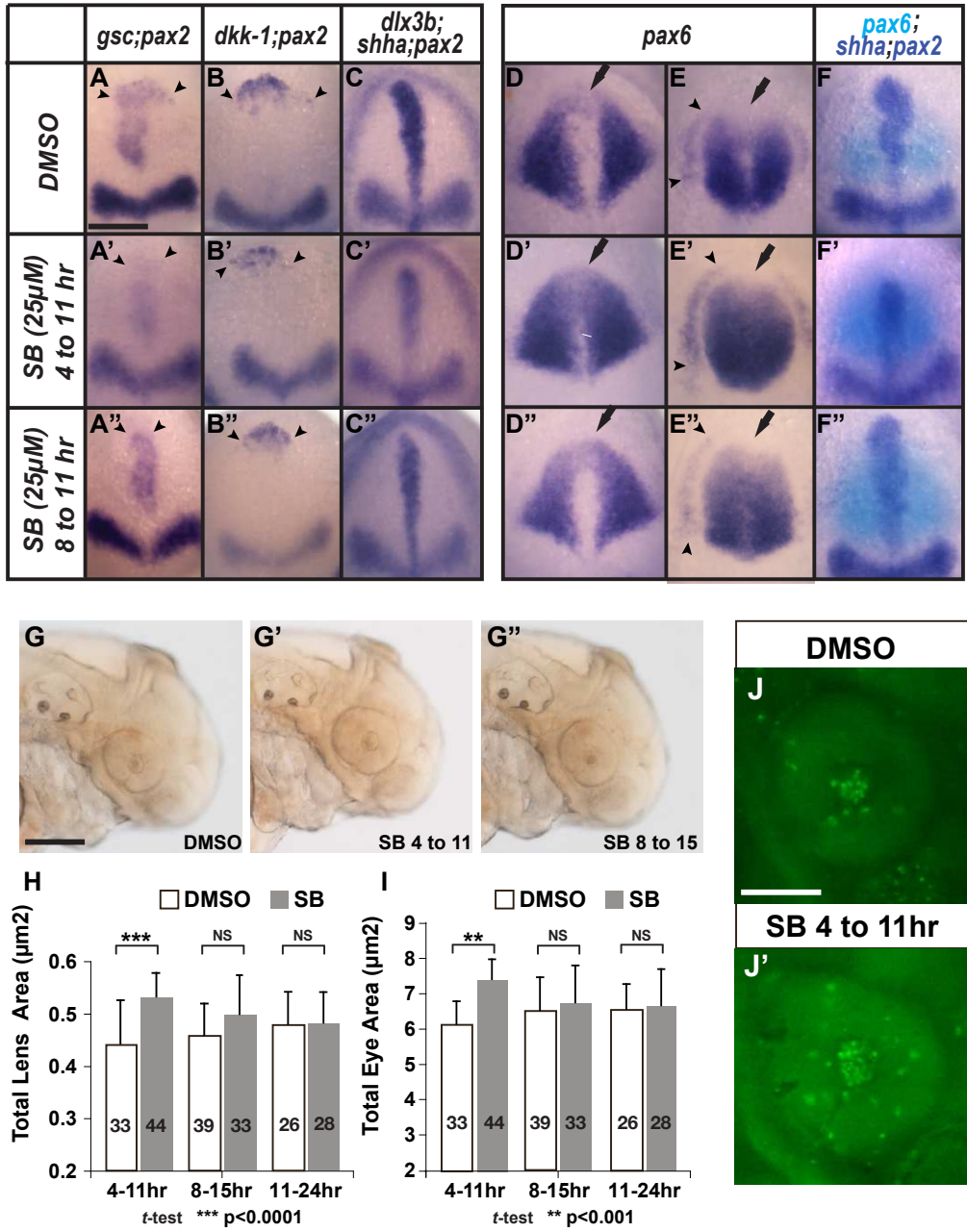


Fig. 3. Decreasing Nodal signaling in the Pachón cavefish reduces anterior expansion of the prechordal plate and increases *pax6* expression in the anterior midline. DMSO control (A-F), early (4 to 11hr, A'-F'), and late (8 to 11hr, A''-F'') of SB431542 (SB, 25 μ M) treated Pachón embryos. (A-B'', tailbud stage) *In situ* hybridization staining shows that reduction of anterior expansion of prechordal plate after the treatment as indicated by *gsc* (A-A'') and *dkk-1* (B-B'') expression (arrowheads). (C-C'', tailbud stage) *shha* expression is also reduced, and the tip of the *shha* domain no longer bend or reach the neural plate border. (D-E'') Correspondingly, the *pax6* expression is increased at the anterior midline (arrows) after the treatment at early tailbud (D-D'') and 1-2 somite stage (E-E''). The anterior midline gap of *pax6* expression has recovered in the treated embryos. The width of the midline gap between the left and right are also reduced. Early treatment (A'-F') is more effective than later treatments (A''-F''). (F-F'', tailbud stage) The two-colour *in situ* hybridization suggest expanded *pax6* (cyan) expression is correlated with the reduced *shha* (dark blue) anterior expression in the SB431542 (SB) treated embryos. (G-G'', 48 hpf) DMSO control (G), early (4 to 11hr, G'), and late (8 to 15hr, G'') of SB (25 μ M) treated embryos at 48 hpf. (H, I) Early SB treatment (4 to 11hr) significantly increased lens and optic cup size. Late SB treatment (8 to 15hr) treatment also has an effect; however the difference is not statistically significant. SB treatment during early somitogenesis does not change the size of lens and optic cup. (J, J', 48 hpf) Acridine orange staining shows SB treatment does not prevent lens apoptosis at 48hr embryos. Scale bars: 250 μ m (A), 150 μ m (G) and 75 μ m (J).

Figure 4

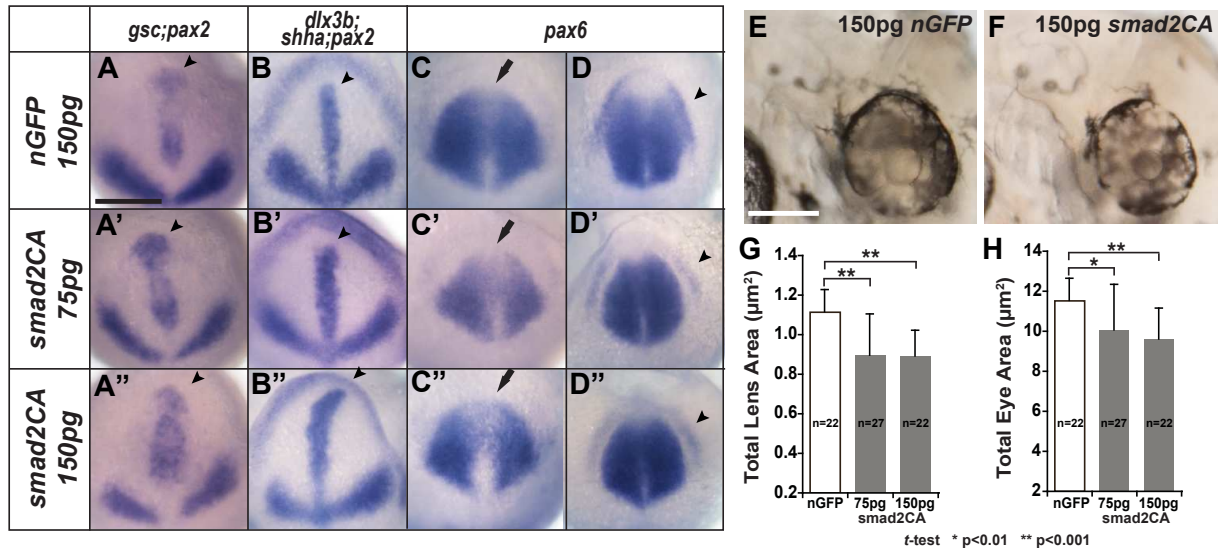


Fig. 4. Increasing nodal signaling in the surface fish enhance the anterior prechordal plate, *shh* expression and decreases *pax6* expression in the anterior midline. 150pg of *nGFP* mRNA as a control (A-D), 75pg (A'-D'), or 150pg (A''-D'') of *smad2CA* injected surface fish embryos. (A-D'', A-C'' early tailbud and D-D'' 1-2 somite stage) *In situ* staining show that the increasing Nodal signaling enhances the anterior expression of *gsc* (A-A'') and *shha* (B-B'') and reduces *pax6* expression (C-D'') in the anterior midline. (E-H, 48 hpf) Lens and Optic cup areas are measured in 48hr embryos. Lens and optic cup size were significantly smaller in *smad2CA* injected embryos versus *nGFP* control mRNA injected fish. Scale bars: 250 μm (A) and 150 μm (E).

Figure 5

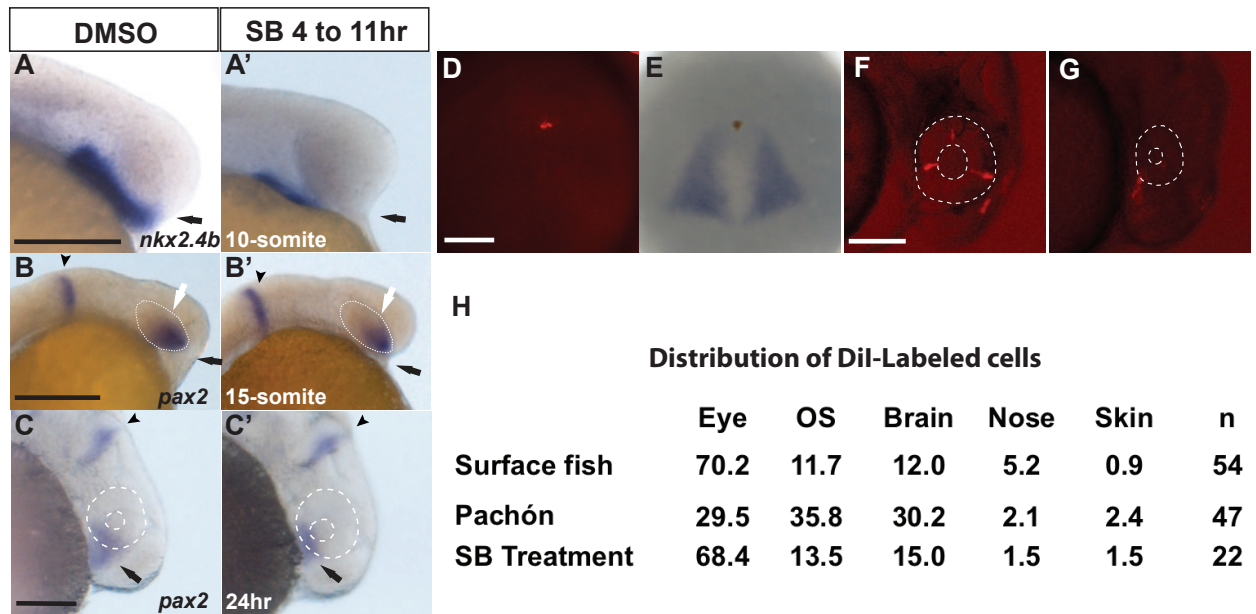


Fig. 5. Optic stalk and hypothalamus were reduced in SB431542 treated cavefish embryos. DMSO control (A-C), early SB431542 (4 to 11hr) treated (A'-C') Pachón embryos. We performed *in situ* hybridizations with hypothalamus marker *nkx2.4b* (A, A') and optic stalk marker *pax2* (B-C'). (A, A', 10-somite stage) At 10-somite stages, the presumptive hypothalamus is smaller and more posteriorly located in the treated embryo (arrows, A, A'). (B, B', 15-somite stage) At 15-somite stages, *pax2* marks in the anterior optic vesicle which is reduced in the treated fish (white-arrows). The optic vesicle is located more anteriorly and reduces part of the anterior hypothalamus in the treated embryos (black-arrows). (C, C', 24 hpf) In the 24hr embryos, the optic stalk is smaller in the SB treated embryos. However, *pax2* expression in the midbrain-hindbrain boundary is not changed (arrowheads). (D, tailbud stage) Dil labelled anterior neural plate at tailbud stage of cavefish embryos. (E, tailbud stage) Dil labelled tailbud cavefish embryos with *pax6* expression in the ANP after conversion of Dil to DAB precipitate and *in situ* hybridization. (F, G, 24hpf) Examples of Dil staining in 24hr embryos after

labelling at tailbud embryos. A surface fish embryo with Dil in the retina (F) and a cavefish embryo with staining in the optic stalk (G). Scale bars: 250 μm (A,B,D) and 150 μm (C,F). (H) The table shows the Dil labelled midline cells are more likely to contribute to the OS (optic stalk) and brain in the cavefish. In the surface fish, these cells are more likely to contribute to the retina. After SB treatment, the distribution of Dil labelled cells in the cavefish is similar to that of the surface fish.

Figure 6

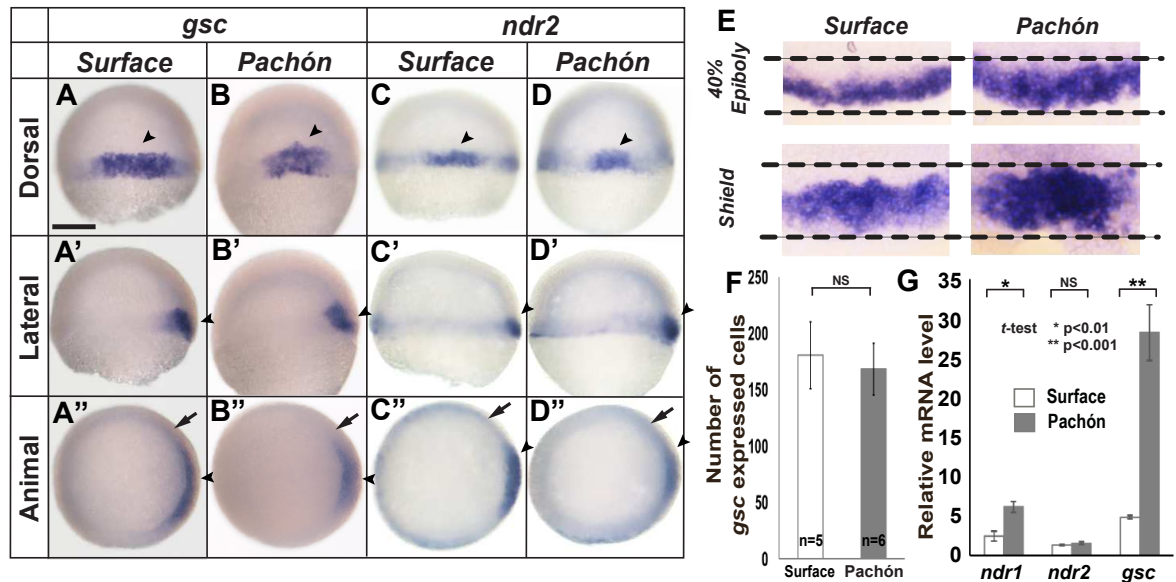


Fig. 6. Modification of the cellular arrangement in the Spemann's organiser. Dorsal (A-D), lateral (A'-D') and animal pole view (A''-D'') of surface fish (A-A'', C-C'') and Pachón cavefish embryos (B-B'', D-D'') at shield stage. (A-B'') Expression pattern of *gsc* (A-B'') and *ndr2* (C-D'') in the Pachón cavefish shows the expression domain in the Spemann's organiser is narrower along the mediolateral axis and wider along the animal-vegetal axis when compared to the surface fish embryos (arrowheads). Germ ring is thicker in the cavefish embryos when compared to the surface fish (arrows). Scale bar: 250 μ m (A). (E) Close-up dorsal view of the *gsc* expression shows the expression domain is wider along the animal-vegetal axis in the cavefish embryos at 40% epiboly and shield stage. (F) Numbers of presumptive prechordal plate cells are not significantly different between the surface fish and cavefish at shield stage. (G) Comparing expression level of two nodal-related genes, *ndr1* and *ndr2*, and *gsc* at shield stage by

quantitative PCR. The *ndr1* expression is two times higher, and *gsc* expression is almost six times higher in the cavefish embryos when compared to the surface fish.

Figure 7

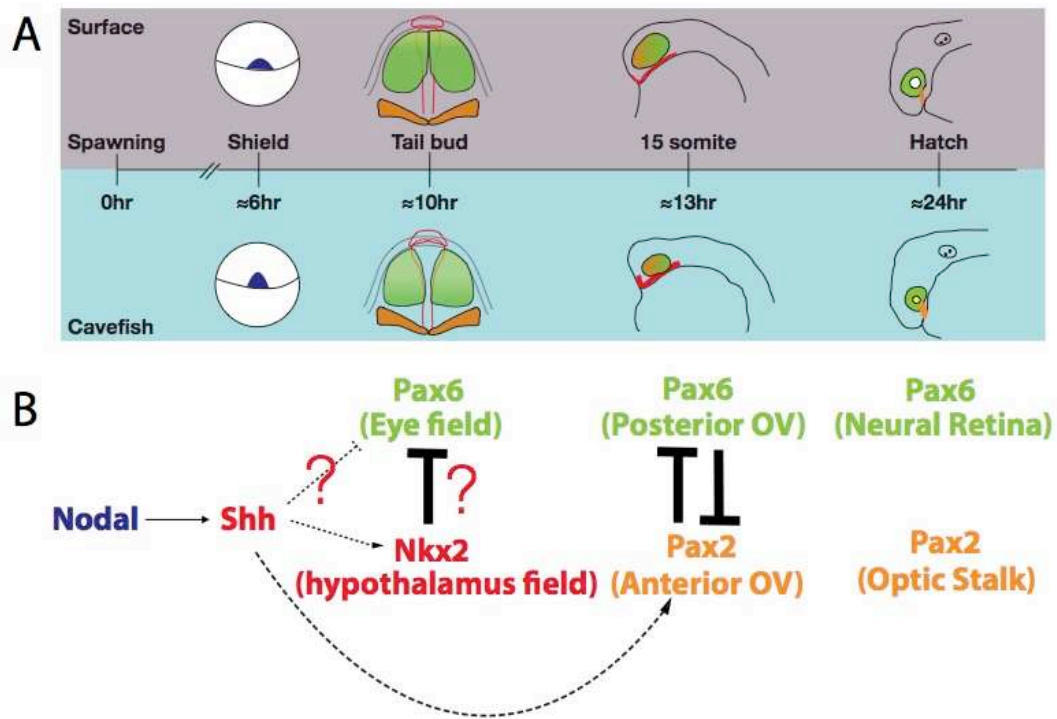


Figure 7 Summary (A) Cellular distribution of *gsc* and *ndr2* expressing cells (dark blue) in Spemann's organiser is modified in cavefish embryos at shield stage. The modification could contribute to the formation of expansion of anterior prechordal plate and small ANP in the cavefish that leads to enhance the *shh* and reduce the *pax6* (green) expression in the anterior midline of the tailbud embryo. The enhanced *shh* induces robust hypothalamus (red) in ventral brain and *pax2* (orange) in anterior optic vesicle during early somitogenesis. At the hatching stage, cavefish embryo has robust optic vesicle (orange) and small optic cup (green) and large hypothalamus. (B) Molecularly, Nodal induces expression of Shh in the anterior midline during gastrulation. The Shh in the prechordal plate controls the expression of Pax6, Nkx2, and Pax2 and the development of the neural retina, hypothalamus and optic stalk, respectively.